Climate regulates the erosional carbon export from the terrestrial biosphere

Robert G. Hilton

Department of Geography, Durham University, DH1 3LD, UK, r.g.hilton@durham.ac.uk, +44 191 33 41970

Abstract: Erosion drives the export of particulate organic carbon from the terrestrial biosphere ($POC_{biosphere}$) and its delivery to rivers. The carbon transfer is globally significant and can result in drawdown of atmospheric carbon dioxide (CO_2) if the eroded $POC_{biosphere}$ escapes degradation during river transfer and sedimentary deposition. Despite this recognition, we lack a global perspective on how the tectonic and climatic factors which govern physical erosion regulate $POC_{biosphere}$ discharge, obscuring linkages between mountain building, climate, and CO_2 drawdown. To fill this deficit, geochemical ($\delta^{13}C$, ^{14}C and C/N), hydrometric (water discharge, suspended sediment concentration) and geomorphic (slope) measurements are combined from 33 globally-distributed forested mountain catchments. Radiocarbon activity is used to account for rock-derived organic carbon and reveals that $POC_{biosphere}$ eroded from mountain forests is mostly <1300 ^{14}C years old. Annual $POC_{biosphere}$ yields are positively correlated with suspended sediment yields, confirming results from Taiwan and a recent global analysis, and are high in catchments with the steepest slopes. Based on these relationships and the global distribution of slope angles (3-arc-second), it is suggested that topography steeper than 10^{o} (16% of the continental area) may contribute ~40% of global $POC_{biosphere}$ erosional flux.

Climate is shown to regulate $POC_{biosphere}$ discharge by mountain rivers, by controlling hydrologically-driven erosion processes. In catchments where discharge measurements are available (8 of the 33) a significant relationship exists between daily runoff (mm day^{-1}) and $POC_{biosphere}$ concentration (mg L^{-1}) ($r = 0.53$, $P < 0.0001$). The relationship can be described by a single power law and suggests a high connectivity between forested hillslopes and mountain river channels. As a result, annual $POC_{biosphere}$ yields are significantly correlated with mean annual runoff ($r = 0.64$, $P < 0.0001$). A shear-stress $POC_{biosphere}$ erosion model is proposed which can explain the patterns in the data. The model allows the climate sensitivity of this carbon flux to be assessed for the first time. For a 1% increase in annual runoff, $POC_{biosphere}$ discharge is predicted to increase by ~4%. In steeper catchments, $POC_{biosphere}$ discharge increases more rapidly with an increase in annual runoff. For reference, the same change in annual runoff is predicted to increase carbon transfers by silicate weathering solute fluxes in mountains by 0.4-0.7%. Depending on the fate of the eroded $POC_{biosphere}$, river export of $POC_{biosphere}$ from mountains may act as an important negative feedback on rising atmospheric CO_2 and increased global temperature. Erosion of carbon from the terrestrial biosphere links mountain building and climate to the geological evolution of atmospheric CO_2, while the carbon fluxes are sensitive to predicted changes in runoff over the coming century.

Keywords: carbon cycling; physical erosion; mountain rivers; radiocarbon; climate and runoff

1. Introduction

Physical erosion can drive the export of carbon from the terrestrial biosphere (Stallard, 1998; Hilton et al., 2012; Galy et al., 2015) and impacts the carbon cycle across a range of timescales. Soils and vegetation of the terrestrial biosphere are estimated to contain ~2000-2900x10^{15} gC at present, >3 times the carbon stock of the pre-industrial atmosphere (Holmén, 2000; Ciais et al., 2013), acting as a major carbon reservoir over 10^0-10^3 years (Sundquist, 1993; Trumbore, 2000). Erosion of particulate organic carbon (POC) from the biosphere ($POC_{biosphere}$) may impact the net size and/or residence time of carbon in this reservoir (Stallard, 1998; Berhe et al., 2007; Galy and Eglinton, 2011; Hilton et al., 2012; Li et al., 2015) and the relatively small size of the atmosphere carbon pool makes it sensitive to these changes on land (Sundquist, 1993; Trumbore, 2000; Carvalhais et al,. 2014). Over longer time periods (10^4-10^6 years, or 'geological'), discharge of $POC_{biosphere}$ by rivers and its delivery to sedimentary environments acts as a major pathway of atmospheric CO_2 drawdown and source of atmospheric O_2 (Berner, 1982; Derry and France-Lanord, 1996; France-Lanord and Derry, 1997) together with marine organic carbon burial (Hayes et al., 1999; Schlunz and Schneider, 2000). Alongside the chemical weathering of silicate minerals by carbonic acid, coupled to calcium carbonate formed from the dissolved weathering products (e.g. Berner et al., 1983; Gaillardet et al., 1999), these processes act to counter geological sources of CO_2 from solid earth degassing via volcanism (Marty and Tolstikhin, 1998) and metamorphism (Becker et al., 2008) and CO_2 release by the oxidation of organic carbon in sedimentary rocks (Berner and Canfield, 1989; Derry and France-Lanord, 1996; Bolton et al., 2006; Hilton et al., 2014).

The climatic and tectonic factors which govern the rates and patterns of physical erosion (e.g. Milliman and Farnsworth, 2011) should be expected to regulate $POC_{biosphere}$ discharge at Earth's surface. Erosion and discharge of $POC_{biosphere}$ by rivers may therefore links mountain building and changes in climate with the geological evolution of atmospheric CO_2. The links between geomorphic processes (erosion and weathering), climate and the inorganic carbon cycle (i.e. silicate weathering) have been widely investigated (e.g. Gaillardet et al., 1999; West et al., 2005; Hilley et al., 2010; West, 2012; Maher and Chamberlain, 2014). High erosion rates are thought to alleviate mineral supply, meaning that silicate weathering rates are controlled by runoff and temperature (West et al., 2005; Gabet and Mudd, 2009; West, 2012; Maher and Chamberlain, 2014). In other words, steep mountains act as Earth's thermostat: they are regions where CO_2 drawdown by silicate weathering is most sensitive to CO_2-induced warming (West et al., 2005; West, 2012; Maher and Chamberlain, 2014), providing a negative feedback which can stabilise long-term climate (Walker et al., 1981; Berner et al., 1983).

In contrast, CO_2 drawdown by the organic carbon cycle and the erosion, riverine transfer of $POC_{biosphere}$ and its burial are much less well understood. We still lack a framework to assess how mountain building and changes in global denudation (Milliman and Farnsworth, 2011; Herman et al., 2013; Larsen et al., 2014a) may impact this carbon flux. Most importantly, the links between climate and $POC_{biosphere}$ discharge by hydrologically-driven erosion processes (e.g. Hilton et al., 2008a; Dhillon and Inamdar, 2013) have not been considered at the global scale (Galy et al., 2015). There is a potential analogy to the CO_2-drawdown associated with silicate weathering. One might expect mountains to play an important role because they have high $POC_{biosphere}$ yields (Hilton et al., 2008b; Hilton et al., 2012), linking tectonic processes to the carbon cycle (Raymo and Ruddiman, 1992). If these $POC_{biosphere}$ yields are regulated by runoff as suggested by a growing number of independent studies (Hilton et al., 2008a; Clark et al., 2013; Smith et al., 2013; Goñi et al., 2013) then there is the potential that erosional export of $POC_{biosphere}$ links climate to the carbon cycle.

Here I fill this research deficit by assessing the global controls and rates of $POC_{biosphere}$ discharge from mountain forests, using data from 33 catchments. Geochemical measurements (^{14}C, $\delta^{13}C$, C/N) are used to account for rock-derived particulate organic carbon (or 'petrogenic' POC, POC_{petro}) and examine the source of biospheric POC. These measurements are combined with measurements of suspended sediment concentration, and daily water discharge data is also available in eight of the catchments. Geomorphic metrics (e.g. slope distributions) are used to help constrain the catchment-scale processes which control $POC_{biosphere}$ erosion. Here, data from eight mountain rivers reveal a remarkably similar positive relationship between $POC_{biosphere}$ concentration (mg L^{-1}) and daily runoff (mm day^{-1}), which can be described well by a single power law relationship. A shear-stress driven $POC_{biosphere}$ erosion model is proposed, which can explain the data. While physical erosion is an important control on $POC_{biosphere}$ yields in mountain catchments (Hilton et al., 2012; Galy et al., 2015) runoff plays a first order role, with catchment average slope moderating this response. Depending on the fate of $POC_{biosphere}$, its erosion from mountain forests can provide a previously unrecognised feedback in the global carbon cycle, linking runoff and CO_2 drawdown. More widespread steep topography makes this feedback mechanism more responsive. Based on these findings, and magnitude of the fluxes involved, it is proposed that the organic carbon cycle may be more important than silicate weathering for moderating Earth's geological carbon cycle, long-term atmospheric CO_2 concentrations and global climate.

2. Materials and Methods

2.1 General Approach

Part of the challenge of understanding the controls on $POC_{biosphere}$ discharge by rivers reflects the input of rock-derived (or 'petrogenic') particulate organic carbon, POC_{petro}, (also referred to as 'fossil POC'). Erosion can contribute POC_{petro} to the solid load of rivers (Kao and Liu, 2000; Blair et al., 2003; Komada et al., 2004; Leithold et al., 2006; Galy et al., 2008a; Hilton et al., 2010), except in catchments draining POC_{petro} poor lithology (e.g. volcanic and plutonic rocks) (Lloret et al., 2013). While recycling of sedimentary POC_{petro} and its supply to rivers was recognised by Meybeck (1993), following earlier quantifications of global organic carbon transfers by rivers (Berner, 1982; Meybeck, 1982; Ittekot, 1988), it wasn't until relatively recent work on mountain rivers that POC_{petro} has started to be systematically accounted for. There is now a global picture, with POC_{petro} important in mountain rivers from Taiwan (Kao and Liu 2000; Hilton et al., 2008a; Hilton et al., 2010), the Himalaya (Galy et al., 2007; Galy et al., 2008a), the Andes (Clark et al., 2013; Bouchez et al., 2014), West Coast of the USA (Blair et al., 2004; Komada et al., 2004; Leithold et al., 2006; Goñi et al., 2013), European Alps (Smith et al., 2013) and New Zealand (Leithold et al., 2006; Hilton et al., 2008b). In order to constrain the modern-day drawdown of atmospheric CO_2, it is vital to account for POC_{petro} inputs in river loads, and quantify only the component eroded from the terrestrial biosphere, $POC_{biosphere}$ (Galy et al., 2007; Hilton et al., 2008a; Galy et al., 2015). While oxidation of POC_{petro} impacts the modern-day carbon cycle by CO_2 release (Hilton et al., 2014), its river transfer and re-burial lengthens its residence time in the crust (Galy et al., 2008a; Hilton et al., 2011a) and does not drawdown modern-day CO_2. Also, without accounting for POC_{petro}, evaluating the geomorphic processes responsible for POC erosion and transfer is not possible: POC_{petro} is closely associated with clastic sediment, whereas $POC_{biosphere}$ is eroded from the surface of forested catchments.

The next challenge having accounted for POC_{petro}, is to measure $POC_{biosphere}$ transport and export by rivers over a range of water discharges and suspended sediment loads (Hilton et al., 2012). These coupled geochemical and hydrometric datasets can estimate $POC_{biosphere}$ discharge (e.g. Kao and Liu, 2000; Hilton et al., 2008a) and reveal the controls $POC_{biosphere}$ discharge (Hilton et al., 2012; Goñi et al., 2013). There are examples of these datasets from individual mountain rivers (Kao and Liu, 1996; Hilton et al., 2008a; Lloret et al., 2013; Smith et al., 2013), paired river catchments with contrasting geomorphic and climatic conditions (Hatten et al., 2012; Goñi et al., 2013) and multiple catchments in Taiwan (Hilton et al., 2012). In addition, recent work has highlighted that catchment-averaged physical erosion rates are a first order control on $POC_{biosphere}$ export by rivers (Hilton et al., 2012; Galy et al., 2015). However, the hydrological/climatic controls (i.e. runoff) which govern clastic sediment routing and export (e.g. Dadson et al., 2003; Larsen et al., 2014a) remain to be assessed at the global scale for $POC_{biosphere}$.

2.2 A Global Mountain River Dataset

The study here uses two approaches: i) individual daily measurements to establish how $POC_{biosphere}$ and POC_{petro} vary with water discharge at the time of sample collection; ii) long-term averages of variables to examine discharges and yields. For (i) there are 33 catchments (Fig. 1a) where the suspended sediment concentration (SSC, mg L^{-1}), organic carbon content ($\%OC_{total}$, weight %), bulk POC concentration (POC, mg L^{-1}, the product of SSC and $\%OC_{total}$) and geochemical measurements to account for POC_{petro} are available (Supplementary Table 1). Out of these, 8 catchments also have water discharge at the time of sample collection. For (ii), there are data from 38 mountain rivers (Supplementary Table 2).

The collection of samples from rivers allows for subsequent geochemical analysis to quantify not only POC concentration, [POC] (mg L^{-1}), but also the petrogenic and biospheric components. I focus on locations where this has been done alongside measurements of ^{14}C activity, referred to here as the 'fraction Modern' (F_{mod}) (Stuiver and Polach, 1977) . F_{mod} values prove an effective means to quantify POC_{petro} inputs (see Section 2.3) and isolate the POC eroded from the terrestrial biosphere, $POC_{biosphere}$ (Galy et al., 2007; Galy et al., 2008a; Hilton et al., 2008a; Hilton et al., 2010; Clark et al., 2013; Hilton et al., 2015). While addition 'total' [POC] measurements (i.e. biospheric + petrogenic) are available for mountain rivers from the literature (e.g. Stallard, 1998; Gomez et al., 2003; Carey et al., 2005; Scott et al., 2006; Goldsmith et al., 2008; Bass et al., 2011; Stallard and Murphy, 2014; Dhillon and Inamdar, 2013) they are not used in this study. The focus is on mountain catchments, rather than large rivers with catchment areas >100,000 km^2 (e.g. Bouchez et al., 2014; Tao et al., 2015), where biological and sedimentary processes within rivers may more strongly modify POC composition (Hedges et al., 2000; Mayorga et al., 2005; Leithold et al., 2016).

Samples were mostly collected from relatively narrow (<50m), turbulent river channels, from the surface of rivers (e.g. Hilton et al., 2008a). In larger channels, samples were collected using depth-integrated sampling (e.g. Mayorga et al., 2005) or by discrete river depth-profile sampling (e.g. Galy and Eglinton, 2011). In total, 32 mountain river catchments have paired SSC, [POC] and F_{mod} measurements (Supplementary Table 1), with 181 individual measurements collated from 17 published papers (Masiello and Druffel, 2001; Komada et al., 2004; Mayorga et al., 2005; Leithold et al., 2006; Alam et al., 2007; Galy et al., 2008a; Galy et al., 2008b; Hilton et al., 2008a; Galy and Eglinton, 2011; Hatten et al., 2012; Clark et al., 2013; Goñi et al., 2013; Lloret et al., 2013; Smith et al., 2013; Kao et al., 2014; Galy et al., 2015; Hilton et al., 2015). Sample sets range from n = 1 to n = 18. In addition, the Capesterre River drains volcanic bedrock for which POC_{petro} can be assumed to be absent (Lloret et al., 2013) meaning that F_{mod} values are not required to quantify $POC_{biosphere}$ and the data set is larger (n=65). The upstream drainage areas of catchments range from 0.7 km^2 to 205,520 km^2, with the majority (n=28) between 50 km^2 and 60,000 km^2.

While the dataset is still limited in terms of overall number of catchments, they do sample mountain forests across continents (Fig. 1a) and biomes/latitudes of boreal/arctic (Peel, Arctic Red), temperate (Erlenbach, Alsea, Siuslaw, Umpqua, Ishikari, Eel, Noyo, Navarro, Waipaoa, Waiapu), sub-tropical (Santa Clara, Karnali, Narayani, Kosi, Fonshan, Lanyang, Liwu, Choshiu, Tsengwen, Kaoping) and tropical (Capesterre, Kosnipata, and Amazon River Basin tributaries). They include mountain rivers which drain ocean islands (e.g. Guadeloupe, Taiwan, New Zealand) and those which feed into major rivers (e.g. the Amazon, Mackenzie, Ganges). Data from mountain rivers are still lacking from high latitudes of South America and from the African continent (Fig. 1a). All rivers drain (meta-) sedimentary rocks, apart from the Capesterre River which drains volcanic rocks.

Alongside SSC, [POC] and F_{mod} measurements, the daily water discharge at the time of sampling, Q_w ($m^3\ s^{-1}$ or $m^3\ day^{-1}$), was sought out wherever possible. 8 of the 33 catchments have paired SSC, [POC], F_{mod} and Q_w measurements, contributing a total of 107 samples. These catchments are in temperate zones (Erlenbach, Alsea, Umpqua, Eel), subtropical (Langyang, Liwu, Choshui) and tropical (Capesterre) settings (Hilton et al., 2008a; Hatten et al., 2012; Goñi et al., 2013; Lloret et al., 2013; Smith et al., 2013; Kao et al., 2014).To compare Q_w in catchments of varying drainage area, A (m^2), the daily runoff, R (mm day^{-1}) has been quantified by normalising Q_w by A.

In addition to daily measurements, annual to decadal estimates of catchment-average suspended sediment yield (t $km^{-2}\ yr^{-1}$) and mean annual runoff (mm yr^{-1}) were collated. Finally, published $POC_{biosphere}$ and POC_{petro} yields (tC $km^{-2}\ yr^{-1}$) are available for 38 mountain rivers (Supplementary Table 2) quantified either using: i) detailed time series sampling and rating curves between Q_w and POC composition and concentration (e.g. Hilton et al., 2011a; Goñi et al., 2013; Lloret et al., 2013; Smith et al., 2013; Taylor et al., 2015); or ii) where suspended sediment yield has already been quantified, and $POC_{biosphere}$ and POC_{petro} concentrations have been combined with that suspended sediment flux (e.g. Hilton et al., 2008b; Galy et al., 2015; Hilton et al., 2015). For the latter method, the relative yields are likely to be accurate (e.g. $POC_{biosphere}$ versus suspended sediment yield), but the absolute values may have larger uncertainty than those quantified from time series sampling (Ferguson, 1986). $POC_{biosphere}$ and POC_{petro} yields were estimated by this approach for the 6 rivers sampled by Leithold et al., (2006) using outputs from the mixing model described below.

2.3 Geochemical Methods, Quantifying $POC_{biosphere}$ Content and its ^{14}C Age

All samples were subject to broadly comparable techniques, with the general procedure comprising: i) filtration at 0.2μm or 0.7μm, removal of samples from filters; ii) homogenisation of samples by agate mill; iii) carbonate removal via acid (HCl) leach (liquid or fumigation); iv) organic carbon concentration, ($\%OC_{total}$) measured by combustion in an Elemental Analyser (EA). For some samples, nitrogen contents (N, %) were also determined via EA and the stable isotope composition of organic carbon ($\delta^{13}C_{org}$, ‰) by continuous flow coupling of EA-Isotope Ratio Mass Spectometry (IRMS). Radiocarbon activities were quantified following combustion and graphitisation by Accelerator Mass Spectrometry and are reported here as the 'fraction Modern' (F_{mod}) normalised to 1950 atmosphere and corrected to –25% $\delta^{13}C_{VPDB}$ based on measured stable isotope ratios (Stuiver and Polach, 1977). Some samples were also analysed for nitrogen isotope composition and biomarker measurements which quantify abundances of organic compounds and their isotopic composition (e.g. Galy and

Eglinton, 2011; Goñi et al., 2013). However these datasets remain limited in geographical extent and are not analysed here.

Previous work has established that in mountain river catchments underlain by sedimentary bedrock, erosion processes result in a mixture of POC_{petro} and $POC_{biosphere}$ (e.g. Kao and Liu, 2000; Komada et al., 2004; Leithold et al., 2006; Galy et al., 2008a; Hilton et al., 2008a). F_{mod} values can be used to quantify the carbon mass fraction of $POC_{biosphere}$ ($f_{biosphere}$) of total POC using a binary mixing model:

$$f_{petro} + f_{biosphere} = 1 \qquad \text{(Eq. 1)}$$

$$F_{mod} = f_{biosphere} \times F_{mod-bio} + f_{petro} \times F_{mod-petro} \qquad \text{(Eq. 2)}$$

where f_{petro} is the fraction of POC_{petro} in each sample, $F_{mod\text{-}bio}$ is the radiocarbon activity of the biospheric POC, and $F_{mod\text{-}petro}$ is the radiocarbon activity of the petrogenic POC. It is reasonable to assume that in sedimentary bedrocks older than 50ka, $F_{mod\text{-}petro} \sim 0$ (i.e. indistinguishable above background). Then, assuming the sediment mixture is well homogenised, the binary mixing model approach of Galy et al., (2008a) predicts the organic carbon content of the total sediment mixture ($\%OC_{total}$):

$$\%OC_{total} = \%OC_{petro} + \%OC_{biosphere} \qquad \text{(Eq. 3)}$$

where these are the weight % of the different components in the same sediment mixture. Equations 1-3 can be combined so that:

$$\%OC_{total} \times F_{mod} = \%OC_{total} \times F_{mod-bio} - \%OC_{petro} \times F_{mod-bio} \qquad \text{(Eq. 4)}$$

If $F_{mod\text{-}bio}$ and $\%OC_{petro}$ are relatively homogeneous in a sample set, equation 4 predicts that a binary mixture should result in a strong linear trend between $\%OC_{total}{\times}F_{mod}$ (y) and $\%OC_{total}$ (x). The gradient of that trend is $F_{mod\text{-}bio}$, which constrains the mean ^{14}C age of $POC_{biosphere}$ (Leithold et al., 2006; Galy and Eglinton, 2011; Bouchez et al., 2014; Tao et al., 2015). The intercept $\%OC_{petro}{\times}F_{mod\text{-}bio}$ constrains the POC_{petro} content of rocks undergoing erosion. If the dataset is well described by this formulation and the assumptions hold, the $f_{biosphere}$ for each sample can be computed (Eq. 2). The concentration of $POC_{biosphere}$, $[POC_{biosphere}]$ mg L^{-1}, is the product of SSC, $\%OC_{total}$ and $f_{biosphere}$.

2.4 Geomorphic parameters

For the 8 catchments with paired SSC, $[POC]_{biosphere}$ and daily R measurements, geomorphic characteristics of the drainage area were quantified to help assess the controls on the erosion and transfer of $POC_{biosphere}$. A 3 arc-second (~90m pixel resolution at the equator) digital elevation model (DEM) derived from the Shuttle Radar Topography Mission elevation data was used, with coverage gaps filled with topographic map data (Larsen et al., 2014a) downloaded from www.viewfinderpanoramas.org. Catchment areas were delineated from filled-DEMs via flow accumulation and flow direction algorithms in ArcGIS. Slope angles were calculated, accounting for the latitudinal dependence on grid cell shape (Z factor). The frequency distribution of elevation and slope values (binned as integers) were quantified (Fig. 1d), apart from the Erlenbach due to its small catchment area (0.74 km^2) in comparison to the DEM resolution. From these distributions, the 16^{th}, 50^{th} and 84^{th} percentile of elevation (Z_{16}, Z_{50} and Z_{84} in meters) and slope angles (θ_{16}, θ_{50} and θ_{84} in degrees) were quantified (Supplementary Table 3).

3. Results

3.1 The Geochemical Composition of POC in Forested Mountain Rivers

The POC samples reveal a large range in F_{mod} values from 0.04 to 1.09, with a mean F_{mod} = 0.59±0.29 (*n* = 181). A large range of $\delta^{13}C_{org}$ values are also evident, from -33.3‰ to -19.7‰, with a mean $\delta^{13}C_{org}$ = -25.5±1.6‰ (Fig. 2a), similar to a global compilation of all riverine POC samples (Marwick et al., 2015). The most ^{14}C-enriched samples (highest F_{mod} values) have $\delta^{13}C_{org}$ values which mostly range between -28‰ and -24.5‰ (Fig. 2a), indicative of young POC fixed from atmospheric CO_2 by C3 plants (Smith and Epstein, 1971) and surface soil horizons beneath C3 vegetation in mountain forest (e.g. Bird et al., 1994; Kao and Lui, 2000). The most ^{14}C-depleted (lowest F_{mod} values) samples have $\delta^{13}C_{org}$ values which mostly range between -26.5‰ and -21.5‰ (Fig. 2a), which is similar to the range of values reported for organic matter in Cenozoic sedimentary rocks (Hayes et al., 1999). The C/N ratios of the eroded particulate organic matter vary from 4.1 to 43 (Fig. 2b), with a mean C/N = 14.0±5.6 (*n*=140). The C/N values at higher F_{mod} (C/N between ~10 and ~35) are consistent with a source from partially degraded C3 biomass and components of recently-derived vegetation. At lower F_{mod} values, variability in bedrock organic matter composition has been shown to play an important role in setting C/N values (Hilton et al., 2010; Clark et al., 2013; Smith et al., 2013). In that context, the Andean catchments (Kosnipata River) appear distinct from other catchments (e.g. Waipaoa) (Fig. 2b). The range of C/N values at low F_{mod} (~5 to~12) are toward the lower range of global compilations of N content in rock-derived organic matter (Holloway and Dahlgren, 2002).

Together, the F_{mod}, $\delta^{13}C_{org}$ and C/N values are consistent with previous observations in forested mountain rivers, suggestive of a mixture of POC_{petro} (F_{mod}~0) and younger $POC_{biosphere}$ (Hilton et al., 2008a; Gomez et al., 2010; Kao et al., 2014). The variable isotopic composition of POC_{petro} (Hayes et al., 1999; Hilton et al., 2010) is evident, based on the range of $\delta^{13}C_{org}$ and C/N values at low F_{mod} values (Fig. 2). In general, POC from catchments with higher average suspended sediment yields can have lower F_{mod} values (Fig. 2a). This has been suggested based on a smaller compilation

(Leithold et al., 2006). However, it is clear that in any one catchment, POC can have a large range of F_{mod} values (Fig. 2a) and a generalisation with catchment-average sediment yield may not be helpful.

The binary mixing model (Eq. 4) describes data from 14 catchments well (Supplementary Table 4). Based on the outputs of this analysis, the $F_{mod\text{-}bio}$ of $POC_{biosphere}$ in mountain rivers mostly ranges between 0.85±0.05 and 1.3±0.3 (Supplementary Table 4). These values correspond to ^{14}C ages from 1330^{+480}_{-450} years to 'modern' (i.e. formed post 1950). One exception is the Narayani River draining high elevations in the Himalaya and Tibet ($F_{mod\text{-}bio}$ = 0.40±0.08, ^{14}C age = 7300^{+1700}_{-1400} yr). Previous work using similar methods identified aged $POC_{biosphere}$, thought to come from high altitude soils in this catchment (Galy and Eglinton, 2011). In addition, the $F_{mod\text{-}bio}$ value for the Peel River at high northern latitudes (note that this was derived from a modified end member mixing analysis in published work) are substantially older ($F_{mod\text{-}bio}$ = 0.49±0.10) due to input of aged-$POC_{biosphere}$ from deep, peat soils (Hilton et al., 2015). This is consistent with ramped pyrolysis ^{14}C analysis of river sediment from the Colville River (Schreiner et al., 2014) and organic compound-specific ^{14}C analyses in high latitude rivers (Feng et al., 2013). The variability in $F_{mod\text{-}bio}$ is important as it reflects the mean residence time of $POC_{biosphere}$ in the landscape (Galy and Eglinton, 2011; Hilton et al., 2015). The values are much older than estimates of $POC_{biosphere}$ turnover time in vegetation and soil, with a global average of 23 years (Carvalhais et al., 2014). However, it is beyond the focus of this manuscript to analyse these patterns further. To do that requires a larger sample set covering a range of climatic conditions and lowland rivers. $F_{mod\text{-}bio}$ values and their uncertainties are used to quantify [$POC_{biosphere}$] and [POC_{petro}] from $f_{biosphere}$ (Eq. 2).

The variability in $\%OC_{total}$ values for Taiwan and New Zealand catchments were not well explained by the binary mixing model outlined in equation 4 (e.g. Liwu River r^2 =0.02, P < 0.25). This is because the assumption that $\%OC_{petro}$ is relatively invariant, does not hold in these locations. This has been highlighted previously in the Liwu River, Taiwan, where the river drains three major geological formations of variable metamorphic grade and age (Beyssac et al., 2007), and $\%OC_{petro}$ varies from ~0.1% to 0.5% (Hilton et al., 2010). Therefore, in these catchments a value of $F_{mod\text{-}bio}$=1.0±0.1 is used to quantify $f_{biosphere}$ following Hilton et al., (2008a), which is similar to the majority of other catchments. However, it may lead to a conservative estimate of $f_{biosphere}$ if aged $POC_{biosphere}$ is important in the upland (Kao et al., 2014). Future work should seek to quantify the age of $POC_{biosphere}$ in mountain river catchments. The analysis of the ^{14}C activity of individual organic compounds such as the vascular plant-derived biomarkers, provides promise (Galy and Eglinton, 2011; Feng et al., 2014; Tao et al., 2015) as does ramped pyrolysis ^{14}C analysis, which can more fully interrogate the age distribution of $POC_{biosphere}$ (Rosenheim and Galy, 2012; Rosenheim et al., 2013)

3.2 Links Between Suspended Sediment, $POC_{biosphere}$ and POC_{petro} Concentrations

Rock-derived POC_{petro} is supplied by the erosion of rocks bearing organic matter. As such, the Capesterre which drains exclusively volcanic bedrock is the only catchment where POC_{petro} is not observed at any time (Lloret et al., 2013). Across the whole dataset, measured [POC_{petro}] was strongly correlated with SSC (r = 0.92, P < 0.0001, n = 167, Fig. 3a). This confirms the premise that POC_{petro} can be part of the clastic sediment load down to low sediment yields of ~53 t km^{-2} yr^{-1} (e.g. the Alsea River). The variability reflects the range in $\%OC_{petro}$ values, which the mixing model predicts varies from <0.01% to ~0.4% (Supplementary Table 4). The Himalayan river samples have lower [POC_{petro}] for a given SSC (Fig. 3a), consistent with their known lower $\%OC_{petro}$ (Galy et al., 2008a; Galy et al., 2008b). In contrast, Taiwan rivers, Andean rivers and those draining the Canadian Rockies (Peel and Arctic Red) have higher $\%OC_{petro}$ (Clark et al., 2013; Hilton et al., 2015). Oxidation of POC_{petro} may play a role in setting variability in $\%OC_{petro}$ (Hilton et al., 2014), but more detailed analysis and discussion is outside the focus of this manuscript.

For the $POC_{biosphere}$, which in these catchments is mainly derived from erosion of surface vegetation and soil from hillslopes, there is a positive correlation between [$POC_{biosphere}$] and SSC (r = 0.55, P < 0.0001). However, it is clear from the patterns in the data that $POC_{biosphere}$ (Fig. 3b) is behaving very differently to POC_{petro} (Fig. 3a). Each catchment has its own positive relationship between [$POC_{biosphere}$] and SSC, but these are shifted depending upon the overall catchment average sediment yield (Fig. 3b). This is expected if increased sediment yield is caused by an increase in overall “erosion depth” and calls for the importance of bedrock landslides (Larsen and Montgomery, 2012). These will act to increase SSC and POC_{petro} (Fig. 3a), but not necessary increase the total surface area undergoing erosion (i.e. the $POC_{biosphere}$). It appears that the ratio of $POC_{biosphere}$ to SSC may thus be a useful proxy to examine overall “erosion depth”. This is an interesting observation which warrants more detailed investigation, however lies outside the scope of the current manuscript. Overall, the erosion and river transport of $POC_{biosphere}$ and POC_{petro} are somewhat decoupled in forested mountain belts (Fig. 3).

3.3 Links Between Daily Runoff, $POC_{biosphere}$ and POC_{petro} Concentrations

When daily runoff (R, mm day^{-1}) is plotted against SSC there is a clear separation of the samples (Fig. 4a). For individual catchments, SSC increases with R, which has been widely reported elsewhere (e.g. Hicks et al., 2004; Milliman and Farnsworth, 2011). However for a given value of daily R, SSC are several orders of magnitude greater in catchments with higher average suspended sediment yield (Fig. 4a). Mountain catchments undergoing higher rates of physical erosion are capable of transporting higher quantities of suspended sediment for a given runoff (Milliman and Syvitski, 1992). Taiwan river catchments experience high rates of tectonic uplift, fluvial incision and bedrock landsliding (Dadson et al., 2003) which can cause much higher SSC for a given R than rivers on the west coast of the US (e.g. Eel River) with lower rates of tectonic uplift (Goñi et al., 2013) or the Capesterre River, Guadeloupe (Lloret et al., 2013) (Fig. 4a). Because POC_{petro} is intimately linked to clastic sediment (Fig. 3a), the same patterns are observed for POC_{petro} versus daily R (Fig. 4b).

When the biospheric organic carbon is examined, there is a stark contrast (Fig. 5). Daily R is significantly correlated with the concentration of $POC_{biosphere}$, [$POC_{biosphere}$] (mg L^{-1}), across the 8 catchments with available hydrometric and geochemical data (r = 0.53, P = 0.0001, n = 107). The samples are well described by a single power law (r^2 = 0.40, Fig. 5). Power law relationships between water discharge and [$POC_{biosphere}$] have been noted before for individual catchments (Hilton et al., 2008a; Hatten et al., 2012; Smith et al., 2013). However, by normalising water discharge by drainage area to R, it appears there may be a common dynamic in the erosion and river transport of $POC_{biosphere}$ from forested mountain rivers. Catchments with the highest median slope angles (Liwu $\theta_{50} = 30^o$ and Choshui $\theta_{50} = 26^o$; Supplementary Table 3) have [$POC_{biosphere}$] values which define the upper range for a given value of R (Fig. 5). In contrast, in the Alsea ($\theta_{50} = 17^o$) and Capesterre ($\theta_{50} = 18^o$) have lower median slope angles and their [$POC_{biosphere}$] values extend the range to lower bounds at a given value of R. Catchments with moderate to high slope angles (Lanyang $\theta_{50} = 23^o$) lie between this range.

3.4 Controls on $POC_{biosphere}$ and POC_{petro} Yields

The $POC_{biosphere}$ yields from mountain river catchments are positively correlated with the suspended sediment yield (r = 0.53, P = 0.0006, n = 38, Fig. 6a) as previously reported for Taiwan (Hilton et al., 2012) and in a recent global compilation (Galy et al., 2015). The global power law relationship of Galy et al., (2015) is consistent with the data compilation here (Fig. 6a) but the trend is different because of the inclusion of lower sediment yield catchments in that dataset (Galy et al., 2015). In addition, the θ_{84} value is positively correlated with suspended sediment yield in this dataset (r = 0.84, P = 0.0002, n = 9), following reported links between catchment slope and sediment yield in larger global compilations (Portenga and Bierman, 2011; Larsen et al., 2014a; Willenbring et al., 2015). θ_{84} is positively correlated with $POC_{biosphere}$ yield, albeit not at the 95% confidence level (r = 0.62 , P = 0.07, n = 9).

The global compilation reveals a more significant correlation between mean annual runoff and $POC_{biosphere}$ yield (r = 0.64, P <0.0001, n = 32, Fig. 6b) than between $POC_{biosphere}$ yield and suspended sediment yield (r = 0.53, P = 0.0006, n = 38). There is weak relationship between suspended sediment yield and mean annual runoff (r = 0.20, P = 0.27, n = 32) suggesting that auto-correlation between variables does not control this relationship. While Stallard (1998) proposed a link between mean annual runoff and total POC yield, that dataset contained considerable variability attributable to the variable input of POC_{petro}. The results highlight for the first time that annual runoff is a major control on $POC_{biosphere}$ yields in mountain river catchments (Fig. 6b).

In terms of rock-derived POC, the strong link between [POC_{petro}] and SSC (Fig. 3a) results in a strong correlation between suspended sediment yield and POC_{petro} yield (r = 0.96, P < 0.0001, n= 38) similar to that reported previously (Hilton et al., 2011; Galy et al., 2015). The relationship is expected if POC_{petro} is an integral part of the clastic sediment (Blair et al., 2003). While high erosion rates can lead to high oxidative weathering fluxes of POC_{petro} as fresh material is exposed (Hilton et al., 2014), overall weathering intensity is low in these settings (Bolton et al., 2006). In other words the ratio of chemical to physical denudation of POC_{petro} is low in mountains. This means that both river POC_{petro} discharge and POC_{petro} oxidative weathering rates can increase with increasing erosion rate (Hilton et al,. 2014). In analogy to suspended sediment yield, POC_{petro} yield is poorly correlated with annual runoff in the study catchments (r = 0.13, P = 0.5, n = 32).

4. Discussion

The export of carbon from mountain forests appears to be regulated by runoff in the study catchments. The global compilation reveals a significant correlation between daily runoff (R) and the concentration of $POC_{biosphere}$ ([$POC_{biosphere}$]) carried by mountain rivers (Fig. 5). The steepness of the catchment may play an important role in moderating this relationship. The behaviour of $POC_{biosphere}$ with daily runoff contrasts starkly with that of the clastic sediment load and POC_{petro} (Fig. 4) and is suggestive of a common set of processes which drive $POC_{biosphere}$ export from forested mountains. If these can be better understood, this may help to explain the observed relationships between longer-term estimates of $POC_{biosphere}$ yield (tC km^{-2} yr^{-1}) and suspended sediment yield (Fig. 6a) (Hilton et al., 2012; Galy et al., 2015) and mean annual runoff (Fig. 6b). In this discussion, a shear-stress erosion model is first proposed to explain the global relationships (Fig. 5). Following this, I explore how climatic factors may regulate $POC_{biosphere}$ discharge from mountains, and assess the wider implications for the global carbon cycle.

4.1 A Shear-Stress Driven $POC_{biosphere}$ Erosion Model

An erosion model is proposed which seeks to explain the data patterns, while providing a framework to assess how runoff (climate) and slope (linked to tectonics) impact $POC_{biosphere}$ discharge (cf. West et al., 2005). The positive relationship between daily R and [$POC_{biosphere}$] (Fig. 5) implies that enhanced flow capacity and/or erosional supply occur with an increase in rainfall intensity. Such erosional export is analogous to the shear-stress formulation of particle mass transfer down slope by fluids (Bagnold, 1966). The discharge of mass by a fluid moving over an erodible surface, q_{POC} [M T^{-1}], can be described as a power law function of the shear-stress exerted by that fluid, τ_b [M L^{-1} T^{-2}]:

$$q_{POC} = \kappa_{POC} \cdot {\tau_b}^{\beta} \qquad \text{(Eq. 5)}$$

where κ_{POC} [$M^{-\beta}$ $L^{\beta+1}$ $T^{2\beta-1}$] and β are positive constants. The formulation assumes that thresholds for entrainment and export of mass (i.e. a critical shear stress) are negligible. For clastic sediment, there have been attempts to incorporate thresholds into this shear-stress erosion model (e.g. Govers, 1990, Tucker and Slingerland, 1997). Here, for simplicity a non-threshold form is used based on the lack of observed threshold for $POC_{biosphere}$ transport (Fig. 5).

The parameters of this erosion model (Eq. 5) are analogous to those discussed in the considerable literature on the stream-power (shear-stress) erosion model (e.g. Howard and Kerby, 1983; Howard et al., 1994; Whipple and Tucker, 1999). The coefficient κ_{POC} can be considered as the 'erodability' of $POC_{biosphere}$ at any given location. Factors which may influence this term include the grain size and relative mobility of $POC_{biosphere}$ (Govers, 1990; Hamm et al., 2008; Wohl et al., 2012; Turowski et al., 2013). Where forest cover is present, the abundance of available $POC_{biosphere}$ as biomass and soil may be less important for κ_{POC}. This is because $POC_{biosphere}$ yields are typically only ~1% of net primary productivity (Hilton et al., 2012; Galy et al., 2015) and so $POC_{biosphere}$ can be considered to be abundant and available for erosion. The exponent β is likely to depend on the specific erosion process operating (Bagnold, 1966; Whipple and Tucker, 1999).

If one assumes the conservation of momentum for a steady and uniform flow, τ_b can be described by:

$$\tau_b = \rho \cdot g \cdot D \cdot S \qquad \text{(Eq. 6)}$$

where ρ is the fluid density [M L^{-3}], g the acceleration due to gravity [L T^{-2}], D the flow depth [L] and S the surface slope (tanθ). With minimal infiltration, the flow depth can be described a function of runoff, R [L T^{-1}], delivered over a period of time, t [T]:

$$\tau_b = \rho \cdot g \cdot R \cdot t \cdot S \qquad \text{(Eq. 7)}$$

The erosional discharge of $POC_{biosphere}$ over this time period, q_{POC} [M T^{-1}], can be quantified using the $POC_{biosphere}$ concentration in the fluid, [$POC_{biosphere}$] [M L^{-3}], and the R delivered over a unit surface area, A [L^2], and described by combining Eqs. 5 and 7 to provide a shear-stress $POC_{biosphere}$ erosion model:

$$q_{POC} = [POC_{biosphere}] \cdot R \cdot A = \kappa_{POC} \cdot (\rho \cdot g \cdot R \cdot t \cdot S)^{\beta} \qquad \text{(Eq. 8)}$$

Rearranging this equation to describe [$POC_{biosphere}$] as a function of R over a set time period relevant to the dataset (t = 1 day) and unit area (A = 1 km^2) gives:

$$[POC_{biosphere}] = \kappa_{POC} \cdot (\rho \cdot g \cdot S)^{\beta} \cdot R^{(\beta-1)} \qquad \text{(Eq. 9)}$$

Working from first principles, a shear-stress erosion model predicts a power law relationship between [$POC_{biosphere}$] and *R* for a given value of κ_{POC} and *S*:

$$[POC_{biosphere}] = \alpha \cdot R^{\gamma} \quad \text{(Eq. 10)}$$

The coefficient α includes two variables: i) κ_{POC}, the 'erodability' of $POC_{biosphere}$; and ii) *S* raised to the power $\beta = (\gamma+1)$. κ_{POC} cannot be examined further with the available data here. One might imagine there could be variability in κ_{POC} which reflects important attributes of the biosphere and soil (for instance, the grain size distribution of organic matter, or the thickness of surface organic-matter rich horizons). Future research should seek to understand whether this is a meaningful (and useful) parameter. *S* certainly does vary across the landscape (e.g. Fig. 1d) and a single value for a catchment can only ever represent this variability. Nevertheless, equation 9 offers an explanation for the power law relationship between *R* and [$POC_{biosphere}$] in the global dataset (Fig. 5). Parametrising the model based on the data from global mountain rivers (Fig. 5) gives $\alpha = 0.052 \pm 0.046$ (units a function of M, L and T raised to powers modified by β) and $\gamma = 1.37 \pm 0.17$.

4.1.1 Sensitivity of the Shear-Stress $POC_{biosphere}$ Erosion Model to Slope and Runoff

To assess how the parameters in the model may reflect reality, first the role of slope angle in the sampled catchments is considered. Differences in slope angle change α (Eqs. 9 and 10), thus modify the power law function between [$POC_{biosphere}$] and *R* (Fig. 5). The Capesterre and Liwu rivers are used to explore an upper and lower bound on the slope angle distributions (Fig. 1, Supplementary Table 3) from 9^o (θ_{16} for Capesterre) to 39^o (θ_{84} for the Liwu), with a mid-value of 24^o. These correspond to *S* values (tanθ) from 0.16-0.81, with a mid-value $S = 0.45$. This range of values is used to modify α, remembering α is proportional to $S^{(\gamma+1)}$ (Eqs. 9 and 10) and in the case of the global dataset $(\gamma+1) = 2.37$. At high slope ($\theta = 39^o$ and $S = 0.81$), α is 3.4 times larger than α at a mid-value of *S* ($\theta = 24^o$ and $S = 0.45$). At low slope ($\theta = 9^o$ and $S = 0.16$), α is 0.07 times the mid-value of *S*.

A 3.4x increase in α, and a 0.07x decrease in α, by changing slope angles from 24^o to 39^o and 24^o to 9^o respectively, can explain the range in the empirical data (Fig. 5). In the Capesterre catchment, [$POC_{biosphere}$] values are generally low for a given daily *R* value compared to other catchments. However, the Capesterre does have steep slopes in the catchment (Fig. 1f), as indicated by its $\theta_{84} = 31^o$ (Supplementary Table 3), and [$POC_{biosphere}$] values in this catchment do reach some of the highest measured values for a given *R* (Fig. 5). The distribution of slope angles can explain the spread in the data for that catchment. The same is true for the Liwu River where slopes are steeper.

The role of annual runoff and annual runoff variability for $POC_{biosphere}$ discharge can be examined using the model (Eq. 8). When historical daily *R* records are used for the Eel River (1959-1980) and Liwu River (1970-1999), the model predicts variability in annual $POC_{biosphere}$ yields which are a function of the annual runoff (Fig. 7a), and the mean annual runoff variability (Fig. 7b). The differences between these catchments reflect the very different magnitude frequency distributions for runoff (Fig. 7c), due to intense runoff events during tropical cyclones which impact the island of Taiwan and the Liwu River (Dadson et al., 2003; Hilton et al., 2008a). Overall, the model outputs explain the positive relationship between $POC_{biosphere}$ yield and mean annual runoff (Fig. 6b).

The purpose of this erosion model is not for quantitative prediction at present, however it is useful to reflect on the $POC_{biosphere}$ discharge predicted from the historical runoff data. For the Liwu River, the $POC_{biosphere}$ erosion model (Eq. 8) predicts a decadal average $POC_{biosphere}$ yield of 36 tC km^{-2} yr^{-1} using the historic R records. This is higher than estimates made by Hilton et al., (2012) of 6.8±2.7 tC km^{-2} yr^{-1} for the same catchment from 2003-2004. That study noted that the calculated yields were probably conservative based on outputs of $POC_{biosphere}$ content from a $\delta^{13}C_{org}$ and N/C mixing model and a yield quantified by a flux-weighted method (Ferguson, 1987). The model does not seem to produce unrealistically high values of [$POC_{biosphere}$], with the three highest daily runoffs in the 30 year record having [$POC_{biosphere}$] = 178 mgC L^{-1}, 217 mgC L^{-1} and 440 mgC L^{-1}. The available data show that values >100 mgC L^{-1} have been measured during lower flow events (Fig. 5) (Hilton et al., 2008a; Smith et al., 2013; Kao et al., 2014). It is possible, that the model can provide robust estimates of $POC_{biosphere}$ yield and suggests that global datasets (Galy et al., 2015) may need to be revised upwards.

4.1.2 Geomorphic Processes which Erode $POC_{biosphere}$ from Mountains

Previous work has discussion the processes which act to erode and transport $POC_{biosphere}$ (and POC_{petro}) in mountain rivers (Leithold et al., 2006; Hilton et al., 2008a; Hilton et al., 2012; Clark et al., 2013; Smith et al., 2013). In light of the observed relationship between daily R and [$POC_{biosphere}$] across the sampled mountain catchments (Fig. 5) and the proposed shear-stress driven erosion mode (Eq. 8) is it useful to summarise some of the key themes here. The key processes are thought to be: i) erosion of $POC_{biosphere}$ from forested hillslopes by runoff-driven processes; ii) erosion of $POC_{biosphere}$ from hillslopes by mass wasting processes, such as shallow and bedrock landslides; and iii) production of fine grained $POC_{biosphere}$ by mechanical attrition of coarser $POC_{biosphere}$. Erosion of $POC_{biosphere}$ from in-channel sources is not thought to be a major source of $POC_{biosphere}$ in mountain rivers, especially at high runoff (Hilton et al., 2008a; Clark et al., 2013). The global dataset can provide new insight as to the commonality of these processes.

Erosion of $POC_{biosphere}$ by runoff-driven processes (i.e. overland flow) can explain the global relationship (Fig. 5) and provides a clear link to a shear-stress driven erosion model. Steep slopes often develop limited regolith (Roering et al., 1999; Calmels et al., 2011; West, 2012; Larsen et al., 2014b) and it is common to find bedrock mantled by thin (<1m) colluvium and soil litter, with plants anchored directly to bedrock exposures. In these locations, bedrock is likely to promote overland flow by its minimal infiltration capacity, rather than by saturation (Horton, 1945). In addition, steep slopes should have a high potential for effective hydrological connectivity, promoting the formation of surface flows (Bracken and Croke, 2007; Gomi et al., 2008). These processes are consistent with the relatively young age of $POC_{biosphere}$ quantified in most of the study catchments (Supplementary Table 4), with surface litter material contributing to erosional fluxes. However, fractures and pathways for fluids to contribute to shallow and deep groundwater are also known to be important in steep mountain catchments (Calmels et al., 2011; Clark et al., 2014) which are unlikely to directly erode $POC_{biosphere}$ from hillslopes.

If the trend between [$POC_{biosphere}$] and R was solely attributed to runoff-driven processes, one would have to invoke that thresholds for overland flow are reached across the full range of sampled R values from 1-100 mm day^{-1} (Fig. 5). While this might seem difficult to justify, it is important to note that the annual $POC_{biosphere}$ yields measured across mountain river catchments typically only equate to ~1% of the available $POC_{biosphere}$ produced by photosynthesis over the same time period (Hilton et al., 2012; Galy et al., 2015). Thus not all sections of hillslopes are required to have passed erosion thresholds. At lower runoff intensity overland flow-driven erosion of $POC_{biosphere}$ may occur only in locations with the steepest slopes. Even in the catchments with moderate θ_{50} (e.g. the Capesterre River, θ_{50}= 18°, Fig. 1f), 17% of the catchment area has slope angles >30°. It is important to note that the lack of apparent runoff threshold for $POC_{biosphere}$ erosion (Fig. 5) may not hold for coarser $POC_{biosphere}$ not sampled here (Turowski et al., 2016). $POC_{biosphere}$ larger than 1 mm may require thresholds to initiate motion, entrain woody debris and clear log-jams from mountain rivers (Wohl, et al., 2009; Wohl and Ogden, 2013; Jochner et al., 2015).

In addition to overland flow, mass wasting processes have the potential to erode $POC_{biosphere}$ (Hilton et al., 2011b; West et al., 2011; Ramos-Scharron et al., 2012; Clark et al., 2016). They are consistent with the link between daily R and [$POC_{biosphere}$] (Fig. 5). Shallow landslide rates may increase under saturated conditions (Roering et al., 2015) and move $POC_{biosphere}$ downslope. Large precipitation events can also trigger numerous landslides (Page et al., 2004; Hilton et al., 2008a) which can be very tightly connected to the river network (West et al., 2011; Clark et al., 2016). Even in the Capesterre River where θ_{50} = 18°, in comparison to θ_{50} = 30° in the Liwu River (Supplementary Table 3), field observations demonstrate that mass wasting events erode $POC_{biosphere}$ from mountain forest (Fig. 1f). The landslide process can also explain the input of older $POC_{biosphere}$ into rivers (Galy and Eglinton, 2011) by eroding into deeper soils or mobilising the entire soil $POC_{biosphere}$ stock. Bedrock landslides harvest $POC_{biosphere}$ across a large range of grain sizes, and completely remove whole tracks of forest (Restrepo et al., 2009). These events are likely to be central for the transfer of coarse $POC_{biosphere}$ and larger woody debris (Wohl et al., 2009; Wohl, 2011; Turowski et al., 2013; Jochner et al., 2015). Coarse $POC_{biosphere}$ fluxes are not often measured, but where they have been measured they can represent a significant component (e.g. West et al., 2011; Turowski et al., 2016). In parallel with this, the production of fine grained (<1mm) $POC_{biosphere}$ through mechanical attrition, akin to abrasion of gravel and pebble bedload clasts (Attal and Lave, 2009) could be important, but remains poorly constrained.

The power law dependence of [$POC_{biosphere}$] and *R* (Fig. 5), in addition to the lack of an apparent threshold in its transport, point to a high degree of connectivity in the hydrological-driven erosion of $POC_{biosphere}$. Steep slopes permit this response and processes which erode and transfer $POC_{biosphere}$ may be very different in catchments with lower slopes ($\theta_{50} < 10^o$). In those locations, the nature of runoff generation during rainfall events will be important (Bracken and Croke, 2007) and one may expect that the runoff control on [$POC_{biosphere}$] may not hold for less steep catchments. In addition, catchments with significant anthropogenic modification may experience a different response. Deforestation may manifest itself in a higher $POC_{biosphere}$ at a given runoff if bare soil is exposed (Bruijnzeel, 2004). The runoff response for agricultural soils, which tend to be <10^o slope, may also enhance $POC_{biosphere}$ transfer and any associated nutrients (Quinton et al., 2010). These issues are outside the current study, but remain significant challenges to understanding the impact of anthropogenic activities on riverine carbon fluxes (Hoffman et al., 2013).

4.2 The Role of Mountains for Global $POC_{biosphere}$ Discharge

A recent compilation of suspended load POC source and flux measurements (i.e. POC finer than ~500 µm), estimated the global $POC_{biosphere}$ discharge by rivers to the oceans as 157^{+74}_{-50} Mt C yr^{-1}, with POC_{petro} discharge of 43^{+61}_{-25} Mt C yr^{-1} (Galy et al., 2015). These estimates go beyond previous estimates of riverine POC discharge (Meybeck, 1993; Ludwig et al., 1996) because they account for both POC from the modern biosphere and that derived from rock. Galy et al., (2015)'s estimates are probably the best we can do at present for $POC_{biosphere}$ smaller than ~500 µm (cf. Wohl and Ogden, 2013; Turowski et al., 2016) based on the available F_{mod} measurements. There are three mountain rivers in the present study which do not contribute to the Galy et al., (2015) compilation (Lanyang, Capesterre, Quebrada, Supplementary Table 2). However, they will not significantly modify the global estimates based on 70 river basins. Therefore, it is not the intention to revise this global discharge estimate, nor apply the shear stress model (Eq. 8), but instead to better constrain how important mountains are globally to $POC_{biosphere}$ and POC_{petro} discharge.

Erosion rate is a first order control on $POC_{biosphere}$ and POC_{petro} discharge (Hilton et al., 2012; Galy et al., 2015) and as sediment production hotspots (Milliman and Syvitski, 1992; Milliman and Farnsworth, 2011) mountain rivers should play an important role in $POC_{biosphere}$ discharge to the oceans. Indeed, mountain rivers of Oceania are estimated to discharge 48 Mt Cyr^{-1} of POC_{total} (biosphere + petrogenic) to the oceans (Lyons et al., 2002). Kao et al., (2014) used geochemical methods similar to those described here to estimate the river $POC_{biosphere}$ discharge for this region (up-scaled from Taiwan) to be 10-40 Mt Cyr^{-1}. To provide new insight founded on the improved understanding of the processes operating (Section 4.1, Fig. 5), the global distribution of topographic slope derived from 3-arc-second DEM is used. A recent analysis has used an empirical relationship between catchment-average slope and denudation rate (derived from detrital cosmogenic radionuclides) and applied it to a global DEM at the same spatial scale (Larsen et al., 2014a; Willenbring et al., 2015). The outputs of this analysis suggest a global physical denudation of 21 Gt yr^{-1}, 19 Gt yr^{-1} corrected for internal drainage networks (Larsen et al., 2014), similar to the estimates of riverine sediment discharge to the oceans (Milliman and Farnsworth, 2011). Regardless of the absolute values, the approach confirms that mountains dominate global physical denudation (Milliman and Syviski, 1992). The outputs of Larsen et al., (2014a) suggest that 66% of physical denudation occurs in landscapes steeper than 10^{o} (3-arc-second DEM), which cover only 15.5% (20.9x10^{6} km^{2}) of the land surface.

To consider POC transfers, global relationships between suspended sediment yield and $POC_{biosphere}$ and POC_{petro} yields (Fig. 6a) are used which have been modelled as power-law relationships (Galy et al., 2015):

$POC_{biosphere}$ yield = 0.081×(Suspended sediment yield)$^{0.56}$ ($r^2 = 0.78$, $P < 0.001$) (Eq. 11)

POC_{petro} yield = 0.0007×(Suspended sediment yield)$^{1.11}$ ($r^2 = 0.82$, $P < 0.001$) (Eq. 12)

These relationships are used to convert sediment yield outputs from Larsen et al., (2014a) to quantify $POC_{biosphere}$ yields per 3 arc-second grid cell globally. Larsen et al., (2014a) place an upper bound on total denudation rates at high slope angles (>46^{o}) at 10 mm yr^{-1}. This is due to the observed divergence of catchment-average slope as a control on physical denudation rate at high slopes (Roering et al., 2000; Ouimet et al., 2009; Portenga and Bierman, 2011; Larsen et al., 2014). The consequence is that the physical denudation rates from Larsen et al., (2014) produce a maximum $POC_{biosphere}$ yield of 30 tC km^{-2} yr^{-1} and POC_{petro} yield of 85 tC km^{-2} yr^{-1} at slopes >46^{o} (which cover <0.001% of the continental area). These values are similar those measured in Taiwan (Hilton et al., 2012) where erosion rates are high globally (Hovius et al., 2000; Dadson et al., 2003) and thus provide a sensible upper bound.

The primary assumption of this approach is that catchment-average slope plays the major role in setting not only suspended sediment discharge (Larsen et al., 2014a), but also $POC_{biosphere}$ and POC_{petro} discharge. This assumption is somewhat justified by the observed link between S_{84} and $POC_{biosphere}$ yield from the mountain catchments compiled here (Section 3.4). Slope also plays an important role in moderating the transport of $POC_{biosphere}$, with steeper catchments transporting more $POC_{biosphere}$ at similar runoff (Fig. 5). Finally, the shear-stress erosion model (Eq. 8) supports the important role of slope for $POC_{biosphere}$ discharge (Section 4.1). However, using only slope to predict $POC_{biosphere}$ discharge will only ever deliver a first order estimate because it does not account for the importance of runoff (Figs. 5 and 6b), nor spatial changes in $POC_{biosphere}$ stocks in biomass and POC_{petro} in rocks. While this may not be important for $POC_{biosphere}$ discharge from forested catchments, where only ~1% of the net primary productivity is typically exported (Hilton et al., 2012; Galy et al., 2015), at high elevations and/or latitudes where $POC_{biosphere}$ stocks are minimal or absent this is relevant. With these caveats in mind, the absolute values returned from this an analysis should be treated with caution. $POC_{biosphere}$ yields may be underestimated in steep, tropical catchments with high runoff (Hilton et al., 2008b), and overestimated in semi-arid/cold settings where $POC_{biosphere}$ stocks are substantially lower. POC_{petro} yields may be overestimated because igneous rocks may contain no organic matter.

Based on the distribution of physical denudation with slope from Larsen et al., (2014a) and the empirical relationships defined by Galy et al., (2015), erosion drives a global $POC_{biosphere}$ discharge of ~140 Mt C yr^{-1} and POC_{petro} discharge ~20 Mt C yr^{-1}. These values are similar but at the lower range of recent estimates (Galy et al., 2015), albeit within the large uncertainty associated with any global extrapolation (Milliman and Farnsworth, 2011). More importantly, the approach suggests that ~40% of the global $POC_{biosphere}$ discharge (~50 Mt C yr^{-1}) and ~70% of the global POC_{petro} discharge (~20 Mt C yr^{-1}) originates from topography steeper than 10^{o} (3-arc-second DEM), which represents 16% of the Earth's continental surface. The analysis quantitatively confirms the role of steep mountains not only in the erosion and supply of clastic sediment (Milliman and Syviski, 1992) and solutes (Larsen et al., 2014a), but also for the discharge of $POC_{biosphere}$ and POC_{petro}. They demonstrate an important link between mountain building and the carbon cycle by the export of $POC_{biosphere}$.

4.2.1. Fate of eroded $POC_{biosphere}$

The role of mountains in the long-term carbon cycle is more pronounced when the fate of eroded $POC_{biosphere}$ is considered. While the transport of sediment and organic matter through fluvial sedimentary systems can be complex (Leithold et al., 2016; Romans et al., 2016), the preservation of organic carbon in marine sediments is strongly linked to the clastic sediment accumulation rate (Berner, 1982; Canfield, 1994; Burdige, 2005; Blair and Aller, 2012). In source-to-sink systems fed by rivers draining mountains, $POC_{biosphere}$ burial efficiencies (quoted as % of the input preserved) have been shown to be very high. In the Bay of Bengal, high sediment loads help promote very efficient $POC_{biosphere}$ burial (close to 100%), delivered by the Ganges and Brahmaputra rivers which drain the Himalaya (Galy et al., 2007). Offshore the mountain island of Taiwan, $POC_{biosphere}$ burial efficiencies have been estimated to be >70% (Kao et al., 2014). The Mackenzie River draining the Canadian Rockies has a moderate erosion rate, but an estimated $POC_{biosphere}$ burial efficiency offshore of ~65% (Hilton et al., 2015).

Available data from global source-to-sink studies compiled by Galy et al., (2015) suggest that $POC_{biosphere}$ burial efficiencies increase from ~20% to close to 100% as suspended sediment yields increase from 10 t km^{-2} yr^{-1} to 10,000 t km^{-2} yr^{-1}. Thus, erosion in steep mountain topography with high sediment yields promotes efficient burial of $POC_{biosphere}$. The potential importance of mountains for terrestrial $POC_{biosphere}$ burial can be assessed if one considers low burial efficiencies of 20% for $POC_{biosphere}$ exported from topography with low slope angles <10° (i.e. 20% of the $POC_{biosphere}$ discharge of 90 Mt C yr^{-1} preserved), and higher burial efficiencies of >70% for landscapes with slopes angles >10° (i.e. 70% of the $POC_{biosphere}$ discharge of 50 Mt C yr^{-1} preserved). Much uncertainty remains, primarily in the fate of $POC_{biosphere}$ in the oceans. Nevertheless, this analysis suggests that catchments with steep topography may account for ~70% of the global CO_2 drawdown by sedimentary burial of terrestrial $POC_{biosphere}$. Future work needs to better constrain both global $POC_{biosphere}$ discharge from mountains and quantify its long-term fate in sedimentary environments.

4.3 Climatic Regulation of $POC_{biosphere}$ Discharge and a Stabilising Feedback in the Earth System

The data from forested mountain rivers suggest runoff regulates $POC_{biosphere}$ discharge over days to years (Figs. 5 & 6b). The formulation of the shear-stress erosion model (Eq. 8) fits with these observations. A link between $POC_{biosphere}$ discharge and runoff is important, as this carbon transfer may be modified by changes in the global patterns and amount of runoff, for which temperature is an important driver (Manabe et al., 2004). To explore this is in a quantitative framework, I use the shear-stress model fit to empirical data (Eq. 10; Fig. 5) which allows the role of climatic factors (e.g. mean annual runoff and runoff variability) to be assessed separately from geomorphic/tectonic factors (slope) . A normalised *R* dataset from one of the study catchments is used (the Liwu River), i.e. keeping the catchment annual variability of *R* the same for this analysis (Fig. 7c).

The analysis predicts that $POC_{biosphere}$ discharge by forested mountain rivers is highly sensitive to mean annual runoff. With a constant $\alpha = 0.519$ defined by the empirical data (Fig. 5), an increase in mean annual runoff from 1500 to 2500 mm yr^{-1} (66% increase) raises the model $POC_{biosphere}$ yield from 11 tC km^{-2} yr^{-1} to 38 tC km^{-2} yr^{-1} (~250% increase) (Fig. 8). In other words, $POC_{biosphere}$ yields increase by ~4% per 1% change in annual runoff. The response of $POC_{biosphere}$ discharge to runoff will also be sensitive to the magnitude-frequency distribution of daily runoff values (Fig. 7b), which can differ markedly amongst mountain catchments (Fig. 7c).

These predictions are important when compared to the silicate weathering CO_2 drawdown mechanism (Gaillardet et al., 1999), which is thought to provide the main feedback which acts to buffer atmospheric CO_2 concentrations over geological time (Walker et al., 1981; Berner et al., 1983). Silicate weathering fluxes from mountain catchments have been proposed to have a climate sensitivity which is higher than less steep parts of Earth's surface (West, 2012; Maher and Chamberlain, 2014).

High rates of physical denudation provide an abundant supply of minerals to soils (Larsen et al., 2014b) and in landslide deposits (Emberson et al., 2016) and chemical weathering rates are set by runoff and temperature which control the reaction kinetics (West et al., 2005). Based on these models (West, 2012; Maher and Chamberlain, 2014), at high denudation rates typical of steep mountains (>1000 t km^{-2} yr^{-1}), a 1% increase in runoff would increase silicate weathering solute fluxes (and CO_2 drawdown) by ~0.4-0.7%. $POC_{biosphere}$ discharge from mountains is much more strongly regulated by runoff (Fig. 8). For the same change in runoff, the shear-tress erosion model (Fig. 8) predicts that $POC_{biosphere}$ discharge increases ~6x to 10x more than silicate weathering solute fluxes.

The fate of the eroded $POC_{biosphere}$ must be considered (Blair and Aller, 2012), but even with a low burial efficiency of 20%, the runoff sensitivity of $POC_{biosphere}$ discharge is still higher than that of silicate weathering in mountains (West, 2012; Maher and Chamberlain, 2014). Erosion of $POC_{biosphere}$ from mountain forest therefore offers a strong feedback to climate via runoff. If runoff and global temperature are linked, this is a mechanisms by which atmospheric CO_2 concentrations may be moderated over geological timescales. The carbon fluxes involved (~50 MtC yr^{-1}) are equivalent to silicate weathering (Gaillardet et al., 1999; Galy et al., 2015). Nevertheless, direct feedbacks between organic carbon burial and climate are not presently considered in Earth System Models which seek to quantify the geological carbon cycle (Berner, 2006; Colbourn et al., 2015).

The stabilising feedback which links $POC_{biosphere}$ discharge to mean annual runoff (and thus GMT) operates most efficiently in the steepest parts of the continents. This can be illustrated by varying α (Eq. 10) to represent different slope angles undergoing erosion (Eq. 8). The absolute size of these fluxes remains very uncertain, but the model predicts that for the same change in annual runoff, $POC_{biosphere}$ discharge from steep catchments (higher $\alpha = 0.062$, which is a 20% increase in α) will increase much more than compared to less steep catchments (lower $\alpha = 0.041$, a 20% decrease in α) (Fig. 8). The process-based model suggests that steep mountain catchments play a critical role in governing carbon transfers from the atmosphere. They are locations where the climate sensitivity of carbon transfers are most pronounced (Fig. 8).

The sensitivity of $POC_{biosphere}$ discharge in mountain catchments to runoff is also important in the context of anthropogenic warming. Projected warming of GMTs by ~2.6-4.8°C by the years 2081-2100 (high emission scenario RCP8.5) (Collins et al., 2013) may increase the transfer of $POC_{biosphere}$ from land to rivers, lakes, reservoirs and the oceans if this comes with an increase in runoff. Climate model predictions are still uncertain, but provide an indication that runoff in rivers may increase by 2.3-6.8% per 1°C of GMT change (Manabe et al., 2004; Maher and Chamberlain, 2014). Therefore, based on the runoff sensitivity from the shear-stress erosion model (Fig. 8), 2°C of warming could increase $POC_{biosphere}$ discharge from steep mountain forest by >20%. While these increases are capable of being sustained by net primary productivity in the majority of river basins (Hilton et al., 2012; Galy et al., 2015), it is unknown whether increased erosional fluxes may lead to enhanced terrestrial carbon storage (e.g. Berhe et al., 2007; Hoffmann et al., 2013; Li et al., 2015), or whether degradation and respiration of $POC_{biosphere}$ may contribute to CO_2 degassing by rivers (Raymond et al., 2013). These remain important directions for future research which require expanded spatial and temporal sampling of rivers and new approaches to model $POC_{biosphere}$ discharge and its fate in river networks.

5. Conclusions

Erosion of mountain forest results in an export of carbon from the terrestrial biosphere. The global fluxes are thought to be significant, but it is not known how climatic factors which govern erosion may regulate this carbon transfer. To provide new insight, I use global measurements of particulate organic carbon (POC) concentration from 33 mountain river catchments, where geochemical analyses of POC (^{14}C, $\delta^{13}C$, C/N) are available alongside hydrometric measurements (daily runoff, suspended sediment concentration, suspended sediment yield) and geomorphic metrics (slope angle distributions). The ^{14}C activity is used to account for inputs of rock-derived, or 'petrogenic', POC_{petro}, and isolate the POC eroded from the terrestrial biosphere ($POC_{biosphere}$). The elemental and stable isotopic compositions of $POC_{biosphere}$ and POC_{petro} vary amongst the sample set, and reflect a mixture of C3 vegetation, partially degraded $POC_{biosphere}$ in soil, and POC_{petro} of variable composition. An end member mixing model is used to quantify $POC_{biosphere}$ and its ^{14}C age. The findings suggest that $POC_{biosphere}$ eroded from mountain forest is generally <1300 ^{14}C years old, with older $POC_{biosphere}$ important in catchments draining very high altitudes and high-latitudes. $POC_{biosphere}$ yields are positively correlated with suspended sediment yield, supporting previous observations and weakly correlated with angle of the steepest slopes in catchments. Based on these relationships, a global 3 arc-second DEM was used to estimate how steep mountain topography contributes to $POC_{biosphere}$ discharge. Topography steeper than 10^o (16% of the continental area) may be responsible for >40% of the global $POC_{biosphere}$ erosion (>70% of the global POC_{petro} erosion). These global flux estimates need to be refined by accounting for climate variability which controls $POC_{biosphere}$ erosion.

The global dataset shows for the first time that a single power law relationship between daily runoff (R, mm day^{-1}), and the concentration of $POC_{biosphere}$ ([$POC_{biosphere}$], mg L^{-1}) can describe the available data from 8 distinct catchments (where $[POC_{biosphere}] = \alpha \cdot R^{\gamma}$ and $\alpha = 0.052 \pm 0.046$ and $\gamma = 1.37 \pm 0.17$; $n = 107$). The pre-factor α appears to be linked to the slope angles of the sampled catchments (Fig. 5). Together the data suggest the combined role of overland-flow driven processes and mass wasting events at high runoff, in addition to high connectivity between hillslopes and channels in these steep landscapes, with abundant $POC_{biosphere}$ available for erosion. A result of this correlation at the daily timescale, is that annual $POC_{biosphere}$ yields (tC km^{-2} yr^{-1}) are positively correlated with annual runoff (Fig. 6b). A shear-stress $POC_{biosphere}$ erosion model can explain the data (Eq. 9) and the model is used to explore how climate regulates $POC_{biosphere}$ discharge. A 1% increase in mean annual runoff results in a model increase of $POC_{biosphere}$ discharge by ~4%. $POC_{biosphere}$ discharge appears to be 6x to10x more responsive to increased runoff than silicate weathering solute fluxes in mountains.

The fate of eroded $POC_{biosphere}$ from mountain catchments remains poorly constrained in most cases, as does the rate of CO_2 release by oxidation of POC_{petro}. Nevertheless, the findings here demonstrate the central role of the organic carbon cycle in linking mountain building and climate to the evolution of atmospheric CO_2 levels over geological timescales. Increased global temperature and runoff is predicted to increase $POC_{biosphere}$ discharge by rivers from mountains (Fig. 8). When coupled to enhanced productivity by the biosphere and replacement of the eroded POC in mountain forest, this represents a stabilising feedback to a warming climate, alongside the silicate weathering feedback which is not as responsive to changing runoff as $POC_{biosphere}$ discharge. The $POC_{biosphere}$ climate-CO_2 feedback may operate most efficiently in the steepest topography, where model outputs show changes in runoff lead to the largest responses in $POC_{biosphere}$ discharge (Fig. 8). Having demonstrated these links for the first time, the major challenge is to now adequately describe these processes in Earth System Models which link environmental change and the carbon cycle and understand how they play a role in the long-term evolution of atmospheric CO_2 concentrations.

6. Acknowledgements

RGH was funded by the Natural Environment Research Council (NERC), UK (NERC New Investigator Grant NE/I001719/1). E. Lloret, E. Leithold, M. Goñi, E. Mayorga, V. Galy and I. Larsen are thanked for making their published data available. A.L. Densmore, A. Galy, M. Goñi, N. Hovius, K. Clark, J. Quinton, J. Turowski, D. Milledge and A.J. West are thanked for discussions on these themes prior to submission, and E. Wohl and the organisers of the 2016 Binghamton Symposium on Connectivity are thanked for the opportunity to contribute this research under the theme of '*Geochemical Connectivity*'. Two reviewers are thanked for their insightful comments which improved the manuscript.

7. References

Alam MJ, Nagao S, Aramaki T, Shibata Y, Yoneda M (2007) Transport of particulate organic matter in the Ishikari River, Japan during spring and summer. *Nuclear Instrum Meth Phys Res B* 259, 513–517.

Attal M, Lavé J (2009) Pebble abrasion during fluvial transport: Experimental results and implications for the evolution of the sediment load along rivers. *J Geophys Res* 114, F04023, doi:10.1029/2009JF001328.

Bagnold RA (1966) An approach to the sediment transport problem from general physics. United States Geological Survey Professional Paper 422I.

Bass AM, Bird MI, Liddell MJ, Nelson PN (2011) Fluvial dynamics of dissolved and particulate organic carbon during periodic discharge events in a steep tropical rainforest catchment. *Limnol Oceanogr* 56(6), 2282–2292.

Becker JA, Bickle MJ, Galy A, Holland T (2008) Himalayan metamorphic CO_2 fluxes: Quantitative constraints from hydrothermal springs. *Earth Planet Sci Lett* 265, 616-629.

Berhe AA, Harte J, Harden JW, Torn MS (2007) The significance of the erosion-induced terrestrial carbon sink. *Bioscience* 57, 337-346.

Berner RA (1982) Burial of organic-carbon and pyrite sulfur in the modern ocean – its geochemical and environmental significance. *Am J Sci* 282, 451–473.

Berner RA (2006) GEOCARBSULF: A combined model for Phanerozoic atmospheric O_2 and CO_2. *Geochim Cosmochim Acta* 70, 5653-5664.

Berner RA, Lasaga AC, Garrels RM (1983) The carbonate–silicate geochemical cycle and its effect on atmospheric carbon dioxide over the past 100 million years. *Am J Sci* 283, 641–683.

Berner RA, Canfield DE (1989) A new model for atmospheric oxygen over Phanerozoic time. *Am J Sci* 289, 333–361.

Beyssac O, Simoes M, Avouac JP, Farley KA, Chen YG, Chan YC, Goffe B (2007) Late Cenozoic metamorphic evolution and exhumation of Taiwan. *Tectonics* 26, TC6001.

Bird MI, Haberle SG, Chivas AR (1994) Effect of altitude on the carbon-isotope composition of forest and grassland soils from Papua New Guinea. *Global Biogeochem Cycles* 8, 13–22.

Blair NE, et al. (2003), The persistence of memory: The fate of ancient sedimentary organic carbon in a modern sedimentary system, *Geochim Cosmochim Acta* 67, 63–73, doi:10.1016/S0016-7037(02)01043-8.

Blair NE, Leithold EL, Aller RC (2004) From bedrock to burial: the evolution of particulate organic carbon across coupled watershed–continental margin systems. *Mar Chem* 92, 141–156.

Blair NE, Aller RC (2012) The fate of terrestrial organic carbon in the marine environment. *Annu Rev Mar Sci* 4, 17.1–17.23.

Bolton EW, Berner RA, Petsch ST (2006) The weathering of sedimentary organic matter as a control on atmospheric O_2: II. Theoretical modeling. *Am J Sci* 306, 575–615.

Bouchez J, et al. (2014) Source, transport and fluxes of Amazon River particulate organic carbon: insights from river sediment depth-profiles. *Geochim Cosmochim Acta* 133, 280–298.

Bracken LJ, Croke J (2007) The concept of hydrological connectivity and its contribution to understanding runoff-dominated geomorphic systems. *Hydrol Process* 21, 1749–1763.

Bruijnzeel LA (2004) Hydrological functions of tropical forests: not seeing the soil for the trees? *Agriculture Ecosystems & Environment* 104, 185-228.

Burbank DW, et al. (1996) Bedrock incision, rock uplift, and threshold hillslopes in the northwestern Himalayas. *Nature* 379, 505–510, doi: 10.1038/379505a0.

Burdige DJ (2005) Burial of terrestrial organic matter in marine sediments: A re-assessment. *Global Biogeochem Cycles* 19, GB4011, doi:10.1029/2004GB002368.

Calmels D, et al. (2011) Contribution of deep groundwater to the weathering budget in a rapidly eroding mountain belt, Taiwan. *Earth Planet Sci Lett* 303, 48– 58, doi: 10.1016/j.epsl.2010.12.032.

Canfield DE (1994) Factors influencing organic carbon preservation in marine sediments. *Chem Geol* 114, 315–329, doi: 10.1016/0009-2541(94)90061-2.

Carey AE, Gardner CB, Goldsmith ST, Lyons WB, Hicks DM (2005) Organic carbon yields from small, mountainous rivers, New Zealand, *Geophys Res Lett* 32, L15404.

Carvalhais N, et al. (2014) Global covariation of carbon turnover times with climate in terrestrial ecosystems, *Nature* 514, 213-217.

Ciais P, et al. (2013) Carbon and Other Biogeochemical Cycles. In: *Climate Change 2013: The Physical Science Basis. Contribution of Working Group I to the Fifth Assessment Report of the Intergovernmental Panel on Climate Change* [Stocker, T.F., D. Qin, G.-K. Plattner, M. Tignor, S.K. Allen, J. Boschung, A. Nauels, Y. Xia, V. Bex and P.M. Midgley (eds.)]. Cambridge University Press, Cambridge, United Kingdom and New York, NY, USA.

Clark KE, et al. (2013) New views on "old" carbon in the Amazon river: Insight from the source of organic carbon eroded from the Peruvian Andes. *Geochem Geophys Geosyst* 14, 1644–1659, doi: 10.1002/ggge.20122.

Clark KE, et al. (2014) The hydrological regime of a forested tropical Andean catchment. *Hydrol Earth Syst Sci* 8, 5377–5397.

Clark KE, et al. (2016) Storm-triggered landslides in the Peruvian Andes and implications for topography, carbon cycles, and biodiversity. *Earth Surface Dynamics* 4, 47-70.

Colbourn G, Ridgwell A, Lenton TM (2015) The time scale of the silicate weathering negative feedback on atmospheric CO_2. *Global Biogeochem Cycles* 29, 583–596.

Collins M, et al. (2013) Long-term Climate Change: Projections, Commitments and Irreversibility. In: *Climate Change 2013: The Physical Science Basis. Contribution of Working Group I to the Fifth Assessment Report of the Intergovernmental Panel on Climate Change* [Stocker, T.F., D. Qin, G.-K. Plattner, M. Tignor, S.K. Allen, J. Boschung, A. Nauels, Y. Xia, V. Bex and P.M. Midgley (eds.)]. Cambridge University Press, Cambridge, United Kingdom and New York, NY, USA.

Dadson SJ, et al. (2003) Links between erosion, runoff variability and seismicity in the Taiwan orogeny. *Nature* 426, 648– 651, doi:10.1038/nature02150

Derry LA, France-Lanord C. (1996) Neogene growth of the sedimentary organic carbon reservoir. *Paleoceanography* 11, 267–257.

Dhillon GS, Inamdar S (2013) Extreme storms and changes in particulate and dissolved organic carbon in runoff: Entering uncharted waters? *Geophys Res Lett* 40, 1322–1327.

Emberson R, Hovius N, Galy A, Marc O (2016) Chemical weathering in active mountain belts controlled by stochastic bedrock landsliding. *Nature Geoscience* 9, 42–45.

Feng X, et al. (2013) Differential mobilization of terrestrial carbon pools in Eurasian Arctic river basins. *Proc Natl Acad Sci USA* 110, 14168–14173.

Ferguson RI (1987) Accuracy and precision of methods for estimating river loads. *Earth Surf Processes Landforms* 12, 95–104.

France-Lanord C, Derry LA (1997) Organic carbon burial forcing of the carbon cycle from the Himalayan erosion. *Nature* 390, 65– 67.

Gabet EJ, Mudd SM (2009) A theoretical model coupling chemical weathering rates with denudation rates. *Geology* 37, 151–154.

Gaillardet JB, Dupré B, Louvat P, Allègre CJ (1999) Global silicate weathering and CO_2 consumption rates deduced from the chemistry of large rivers. *Chem Geol* 159, 3–30.

Galy V, et al. (2007) Efficient organic carbon burial in the Bengal fan sustained by the Himalayan erosional system. *Nature* 405, 407–410.

Galy V, Beyssac O, France-Lanord C, Eglinton TI (2008a) Recycling of graphite during Himalayan erosion: A geological stabilization of carbon in the crust. *Science* 322, 943–945, doi:10.1126/science.1161408.

Galy V, France-Lanord C, Lartiges B (2008b) Loading and fate of particulate organic carbon from the Himalaya to the Ganga–Brahmaputra delta. *Geochim Cosmochim Acta* 72, 1767–1787.

Galy V, Eglinton TI (2011) Protracted storage of biospheric carbon in the Ganges–Brahmaputra basin. *Nature Geosci* 4, 843–847, doi: 10.1038/ngeo1293.

Galy V, Peucker-Ehrenbrink B, Eglinton T (2015) Global carbon export from the terrestrial biosphere controlled by erosion. *Nature* 521, 204–207.

Goldsmith ST, et al. (2008) Extreme storm events, landscape denudation, and carbon sequestration: Typhoon Mindulle, Choshui River, Taiwan. *Geology* 36, 483–486, doi: 10.1130/G24624A.

Gomez B, et al. (2003) Production, storage and output of particulate organic carbon: Waipaoa River Basin, New Zealand. *Water Resour Res* 39(6),1161, doi:10.1029/2002WR001619.

Gomez B, Baisden WT, Rogers KM (2010) Variable composition of particle‐bound organic carbon in steepland river systems. *J Geophys Res* 115, F04006, doi:10.1029/2010JF001713.

Gomi T, Sidle RC, Miyata S, Kosugi K, Onda Y (2008) Dynamic runoff connectivity of overland flow on steep forested hillslopes: Scale effects and runoff transfer. *Water Resour Res* 44, W08411, doi:10.1029/2007WR005894.

Goñi MA, Hatten JA, Wheatcroft RA, Borgeld JC (2013) Particulate organic matter export by two contrasting small mountainous rivers from the Pacific Northwest, U.S.A. *J Geophys Res Biogeosci* 118, 1-23.

Govers G (1990) Empirical relationships for the transport capacity of overland flow. *Int Assoc Hydrol Sci Pub* 189, 45-63.

Hamm NT, Dade WB, Renshaw CE (2011) Fine particle deposition to porous beds. *Water Resour Res* 47, W11508, doi:10.1029/2010WR010295.

Hatten JA, Goñi MA, Wheatcroft RA (2012) Chemical characteristics of particulate organic matter from a small mountainous river in the Oregon Coast Range, USA. *Biogeochem* 107, 43-66.

Hayes JM, Strauss H, Kaufman AJ (1999) The abundance of ^{13}C in marine organic matter and isotopic fractionation in the global biogeochemical cycle of carbon during the past 800 Ma. *Chem Geol* 161, 103–125.

Hedges JI, et al. (2000) Organic matter in Bolivian tributaries of the Amazon River: A comparison to the lower mainstream. *Limnol Oceanogr* 45, 1449–1466.

Herman F, et al. (2013) Worldwide acceleration of mountain erosion under a cooling climate. *Nature* 504, 423-426.

Hicks DM, Gomez B, Trustrum NA (2004) Event suspended sediment characteristics and the generation of hyperpycnal plumes at river mouths: East coast continental margin, North Island, New Zealand. *J Geol* 112, 471– 485.

Hilley GE, Chamberlain CP, Moon S, Porder S, Willett SD (2010) Competition between erosion and reaction kinetics in controlling silicate-weathering rates. *Earth Planet Sci Lett* 293, 191–199.

Hilton RG, et al. (2008a) Tropical-cyclone-driven erosion of the terrestrial biosphere from mountains. *Nature Geosci* 1, 759–762, doi: 10.1038/ngeo333.

Hilton RG, Galy A, Hovius N (2008b) Riverine particulate organic carbon from an active mountain belt: Importance of landslides. *Global Biogeochem Cycles* 22, GB1017, doi:10.1029/2006GB002905.

Hilton RG, Galy A, Hovius N, Horng MJ, Chen H (2010) The isotopic composition of particulate organic carbon in mountain rivers of Taiwan. *Geochim Cosmochim Acta* 74, 3164–3181, doi:10.1016/j.gca.2010.03.004.

Hilton RG, Galy A, Hovius N, Horng MJ, Chen H (2011a) Efficient transport of fossil organic carbon to the ocean by steep mountain rivers: An orogenic carbon sequestration mechanism. *Geology* 39, 71–74, doi:520 10.1130/G31352.1.

Hilton RG, Meunier P, Hovius N, Bellingham P, Galy A (2011b) Landslide impact on organic carbon cycling in a temperate montane forest. *Earth Surf Process Landf* 36, 1670–1679, doi: 10.1002/esp.2191.

Hilton RG, et al. (2012) Climatic and geomorphic controls on the erosion of terrestrial biomass from subtropical mountain forest. *Global Biogeochem Cy* **26**, GB3014.

Hilton RG, Gaillardet J, Calmels D, Birck JL (2014) Geological respiration of mountains revealed by the trace element rhenium. *Earth Planet Sci Lett* 403, 27-36.

Hilton RG, et al. (2015) Erosion of organic carbon in the Arctic as a geological carbon dioxide sink. *Nature*.

Hoffmann T, et al. (2013) Humans and the missing C-sink: Erosion and burial of soil carbon through time. *Earth Surf Dynam* 1, 45-52.

Holloway JM, Dahlgren RA (2002) Nitrogen in rock: Occurrences and biogeochemical implications. *Global Biogeochem Cycles* 16, 1118.

Holmén K (2000) The global carbon cycle, in *Earth System Science from Biogeochemical Cycles to Global Change, Int. Geophys. Ser.*, vol. 72, edited by M. C. Jacobson et al., pp. 282–309, Elsevier Academic Press, London, UK.

Horton RE (1945) Erosional development of streams and their drainage basins; hydrophysical approach to quantitative morphology. *Geological society of America bulletin* 56, 275-370.

Hovius N, Stark CP, Allen PA (1997) Sediment flux from a mountain belt derived by landslide mapping. *Geology* 25, 231–234.

Hovius N, Stark CP, Chu HT, Lin JC (2000) Supply and removal of sediment in a landslide-dominated mountain belt: Central Range, Taiwan. *J Geol* 108, 73– 89.

Howard AD, Kerby G (1983) Channel changes in Badlands. *Geol Soc Am Bulletin* 94, 739-752.

Howard AD, Seidla MA, Dietrich WE (1994) Modeling fluvial erosion on regional to continent scales. *J Geophys Res* 99, 13,971-13,986.

Ittekot V (1988) Global trends in the nature of organic matter in river suspensions. *Nature* 332, 436–438.

Jochner M, Turowski JM, Badoux A, Stoffel M, Rickli C (2015) The role of log jams and exceptional flood events in mobilizing coarse particulate organic matter in a steep headwater stream. *Earth Surf Dynam* 3, 311-320.

Kao SJ, Liu KK (2000) Stable carbon and nitrogen isotope systematics in a human-disturbed watershed (Lanyang-Hsi) in Taiwan and estimation of biogenic organic carbon and nitrogen fluxes. *Global Biogeochem Cycles* 14(1), 189–198.

Kao SJ, et al. (2014) Preservation of terrestrial organic carbon in marine sediments offshore Taiwan: mountain building and atmospheric carbon dioxide sequestration. *Earth Surf Dynam* 2, 127–139.

Komada T, Druffel ERM, Trumbore SE (2004) Oceanic export of relict organic carbon by small mountainous rivers. *Geophys Res Lett* 31, 1–4.

Larsen IJ, Montgomery DR (2012) Landslide erosion coupled to tectonics and river incision. *Nature Geosci* 5, 468–473.

Larsen IJ, Montgomery DR, Greenberg HM (2014a) The contribution of mountains to global denudation. *Geology* 42, 527–530.

Larsen IJ, et al. (2014b) Rapid Soil Production and Weathering in the Southern Alps, New Zealand. *Science* 343, 637-640.

Leithold EL, Blair NE, Perkey DW (2006) Geomorphologic controls on the age of particulate organic carbon from small mountainous and upland rivers. *Global Biogeochem Cycles* 20, GB3022.

Leithold EL, Blair NE, Wegmann KW (2016) Source to sink sedimentary systems and the global carbon burial: A river runs through it. *Earth-Science Reviews*153, 7–29.

Li Y, et al. (2015) Sustained high magnitude erosional forcing generates an organic carbon sink: Test and implications in the Loess Plateau, China. *Earth Planet Sci Lett* 411, 281–289.

Lloret E, et al. (2013) Dynamic of particulate and dissolved organic carbon in small volcanic mountainous tropical watersheds *Chem Geol* 351, 229–244.

Ludwig W, Probst JL, Kempe S (1996) Predicting the oceanic input of organic carbon by continental erosion. *Global Biogeochem Cycles* 10(1), 23–41.

Lyons WB, Nezat CA, Carey AE, Hicks DM (2002) Organic carbon fluxes to the ocean from high-standing islands. *Geology* 30, 443–446.

Maher K, Chamberlain CP (2014) Hydrologic regulation of chemical weathering and the geologic carbon cycle. *Science* 343, 1502- 1504.

Manabe S, Wetherald RT, Milly PCD, Delworth TL, Stouffer RJ (2004) Century-scale change in water availability: CO_2 -quadrupling experiment. *Clim Change* 64, 59–76.

Marty B, Tolstikhin IN (1998) CO_2 fluxes from mid-ocean ridges, arcs and plumes. *Chem Geol* 145, 233-248.

Marwick TR, et al. (2015) The age of river-transported carbon: A global perspective. *Global Biogeochem Cycles* 29, 122–137.

Masiello CA, Druffel ERM (2001) Carbon isotope geochemistry of the Santa Clara River. *Global Biogeochem Cycles* 15, 407-416.

Mayorga E, et al. (2005) Young organic matter as a source of carbon dioxide outgassing from Amazonian rivers. *Nature* 436, 538–541, doi:10.1038/nature03880.

Meybeck M (1982) Carbon, nitrogen and phosphorus transport by world rivers. *Am J Sci* 282, 401-450.

Meybeck M (1993) C, N, P, and S in rivers: From sources to global inputs, in *Interactions of C, N, P and S Biogeochemical Cycles and Global Change*: Berlin, pp. 163–193, Springer, New York.

Milliman JD, Farnsworth KL (2011) *River Discharge to the Coastal Ocean: A Global Synthesis*, Cambridge University Press, Cambridge, U. K.

Milliman JD, Syvitski JPM (1992) Geomorphic/tectonic control of sediment discharge to the Ocean: The importance of small mountainous rivers. *J Geol* 100, 525– 544.

Ouimet WB, Whipple KX, Granger DE (2009) Beyond threshold hillslopes: Channel adjustment to base-level fall in tectonically active mountain ranges. *Geology* 37, 579-582.

Page M, Trustrum N, Brackley H, Baisden T (2004) Erosion-related soil carbon fluxes in a pastoral steepland catchment, New Zealand. *Agriculture, Ecosystems and Environment* 103, 561–579.

Petsch ST, Berner RA, Eglinton TI (2000) A field study of the chemical weathering of ancient sedimentary organic matter. *Org Geochem* 31, 475–487.

Portenga EW, Bierman, PR (2011) Understanding Earth's eroding surface with ^{10}Be. *GSA Today* 21, 4–10.

Quinton JN, Govers G, Van Oost K, Bardgett RD (2010) The impact of agricultural soil erosion on biogeochemical cycling. *Nature Geosci* 3, 311–314.

Ramos Scharrón CE, Castellanos EJ, Restrepo C (2012) The transfer of modern organic carbon by landslide activity in tropical montane ecosystems. *J Geophys Res* 117, G03016.

Raymo ME, Ruddiman WF (1992) Tectonic forcing of late Cenozoic climate. *Nature* 359, 117– 122.

Raymond P, et al. (2013) Global carbon dioxide emissions from inland waters. *Nature* 503, 355-359.

Restrepo C, et al. (2009) Landsliding and its multiscale influence on mountainscapes. *Bioscience* 59, 685–698, doi:10.1525/bio.2009.59.8.10.

Roering JJ, Kirchner JW, Dietrich WE (1999) Evidence for nonlinear, diffusive sediment transport on hillslopes and implications for landscape morphology. *Water Resour Res* 35, 853–870.

Roering JJ, Kirchner JW, Dietrich WE (2001) Hillslope evolution by nonlinear, slope-dependent transport: Steady-state morphology and equilibrium adjustment timescales. *J Geophys Res* 106, 16,499-16,513.

Roering JJ, et al. (2015) Beyond the angle of repose: A review and synthesis of landslide processes in response to rapid uplift, Eel River, Northern California. *Geomorphology* 236, 109–131.

Romans BE, Castelltort S, Covault JA, Fildani A, Walsh JP (2016) Environmental signal propagation in sedimentary systems across timescales. *Earth Science Reviews* 153,7–29.

Rosenheim BE, Galy V (2012) Direct measurement of riverine particulate organic carbon age structure. *Geophys Res Lett* 39, L19703.

Rosenheim BE, et al. (2013) River discharge influences on particulate organic carbon age structure in the Mississippi/Atchafalaya River System. *Global Biogeochem Cycles* 27, 1-13.

Schlunz B, Schneider RR (2000) Transport of terrestrial organic carbon to the oceans by rivers: re-estimating flux- and burial rates. *Int J Earth Sci* 88, 599–606.

Schreiner KM, Bianchi TS, Rosenheim BE (2014) Evidence for permafrost thaw and transport from an Alaskan North Slope watershed. *Geophys Res Lett* 41, 1-10.

Scott DT, et al. (2006) Localized erosion affects national carbon budget. *Geophys Res Lett* 33, L01402,

Smith JC, et al. (2013) Runoff-driven export of particulate organic carbon from soil in temperate forested uplands. *Earth Planet Sci Lett* 365, 198–208.

Stallard RF (1998) Terrestrial sedimentation and the carbon cycle: Coupling weathering and erosion to carbon burial. *Global Biogeochem Cy* 12(2), 231–257.

Stallard RF, Murphy SF (2014) A unified assessment of hydrologic and biogeochemical responses in research watersheds in Eastern Puerto Rico using runoff–concentration relations. *Aquat Geochem* 20,115–139.

Stuiver M, Polach HA (1977) Discussion: Reporting of ^{14}C data. *Radiocarbon* 19, 355–363.

Sundquist ET (1993) The global carbon dioxide budget. *Science* 259, 934–941.

Tao S, Eglinton TI, Montluçon DB, McIntyre C, Zhao M (2015) Pre-aged soil organic carbon as a major component of the Yellow River suspended load: Regional significance and global relevance. *Earth Planet Sci Lett* 414, 77–86.

Taylor PG, et al. (2015) Organic forms dominate hydrologic nitrogen export from a lowland tropical watershed. *Ecology* 96, 1229–1241.

Trumbore S (2000) Age of soil organic matter and soil respiration: Radiocarbon constraints on belowground C dynamics. *Ecological Applications* 10, 399–411.

Tucker GE, Slingerland RL (1997) Drainage basin response to climate change. *Water Resour Res* 33, 2031-2047.

Turowski JM, et al. (2013) The mass distribution of coarse particulate organic matter exported from an Alpine headwater stream. *Earth Surf Dynam* 1, 1–11.

Turowski JM, Hilton RG, Sparkes R (2016) Decadal carbon discharge by a mountain stream is dominated by coarse organic matter. *Geology* 44, 27–30.

Walker JCG, Hays PB, Kasting JF (1981) A negative feedback mechanism for the long-term stabilisation of Earth's surface temperature. *J Geophys Res* 86 9776– 9782.

West AJ, Galy A, Bickle M (2005) Tectonic and climatic controls on silicate weathering. *Earth Planet Sci Lett* 235, 211–228, doi:10.1016/j.epsl.2005.03.020.

West AJ, et al. (2011) Mobilization and transport of coarse woody debris by large storms. *Limnol Oceanogr* 56, 77–85, doi:10.4319/lo.2011.56.1.0077.

West AJ (2012) Thickness of the chemical weathering zone and implications for erosional and climatic drivers of weathering and for carbon cycle feedbacks. *Geology* 40, 811–814.

Whipple KX, Tucker GE (1999) Dynamics of the stream-power river incision model: Implications for height limits of mountain ranges, landscape response timescales, and research needs. *J Geophys Res* 104, 17,661-17,674.

Willenbring JK, Codilean AT, Ferrier KL, McElroy B, Kirchner JW (2015) Short Communication: Earth is (mostly) flat, but mountains dominate global denudation: apportionment of the continental mass flux over millennial time scales, revisited. *Earth Surf Dynam Discuss* 2, 1-17.

Wohl E, Ogden F, Goode J (2009) Episodic wood loading in a mountainous neotropical watershed. *Geomorphology* 111, 149-159.

Wohl E (2011) Threshold-induced complex behavior of wood in mountain streams. *Geology* 39, 587–590.

Wohl E, Dwire K, Sutfin N, Polvi L, Bazan R (2012) Mechanisms of carbon storage in mountainous headwater rivers. *Nature Communications* 3, 1263.

Wohl E, Ogden FL (2013) Organic carbon export in the form of wood during an extreme tropical storm, Upper Rio Chagres, Panama. *Earth Surf Process Landforms* 38, 1407-1416.

8. Figure Captions

Figure 1: Mountain river catchments used in this study. A) Datasets from forested mountain river catchments used in this study (Supplementary Tables 1 and 2). **B)** and **C)** Examples of the quantification of catchment geomorphic characteristics (Supplementary Table 3) for the Liwu River, Taiwan (**B**), and Capesterre River, Guadeloupe (**C**), with sampling points and gauging stations shown as a white star, and the catchment elevation given. **D)** Examples of slope angle distribution determined from 3 arc-second Digital Elevation Model (Supplementary Table 3). **E)** Mountain forest and steep landscape of the Liwu River showing evidence for recent bedrock landslides. **F)** Tropical forest in the Capesterre River (photo used with permission of François Beauducel, IPG, Paris), with patchwork of regrowth on steep hillslopes evidence of recent mass wasting events.

Figure 2: Geochemistry of particulate organic carbon (POC) carried by forested mountain rivers. A) Fraction Modern (F_{mod}, from ^{14}C activity) versus the stable isotopic composition of POC ($\delta^{13}C_{org}$, permil), with individual catchments labelled and coloured based on their suspended sediment yield (t km^{-2} yr^{-1}) (light grey = no published estimate) (Supplementary Table 1), where: P = Peel, AR = Arctic Red, Er = Erlenbach, Al = Alsea, Si = Siuslaw, Um = Umpqua, Ish = Ishikari, Ee = Eel, No =

Noyo, Na = Navarro, SC = Santa Clara, Ka = Karnali, Ny = Narayani, Ko = Kosi, F = Fonshan, La = Langyang, Li = Liwu, W = Wu, Ch = Choshui, T = Tsengwen, G = Gaoping, Uc = Ucayali, Ur = Urubamna, T= Tambo, KSP = Kosnipata – San Pedro, KW = Kosnipata – Wayqecha, Ap = Apurimac, Sa = Salcca, V = Vilcanota, Z = Zongo, Wa = Waiapu, Wp = Waipaoa. **B)** As part A, but for the organic carbon to nitrogen ratio (C/N) of the particulate organic matter. Regions corresponding to the expected compositions of biospheric POC and rock-derived, 'petrogenic' POC for forested mountain river catchments are shown as rectangles and are discussed in the main text. Analytical uncertainties are smaller than the point size.

Figure 3: $POC_{biosphere}$ and POC_{petro} versus suspended sediment concentration. A) Rock-derived POC concentration, [POC_{petro}] (mg L^{-1}) versus daily runoff (mm day^{-1}) as a function of suspended sediment concentration, [SSC] (mg L^{-1}), with points labelled by catchment and coloured based on their catchment average suspended sediment yield (as per Fig. 2) (Supplementary Table 1). Note, the Capesterre catchment has volcanic bedrock bearing no POC_{petro} and so does not appear on this plot. **B)** Concentration of POC eroded from the terrestrial biosphere, [$POC_{biosphere}$] (mg L^{-1}) versus [SSC], labelled the same way as part **A**. Grey filled symbols are catchments with no yield information. Uncertainties are derived from the mixing model outputs (Supplementary Table 4) and shown as grey whiskers if larger than the point size.

Figure 4: Daily runoff versus suspended sediment and POC_{petro} concentration. A) Suspended sediment concentration ([SSC], mg L^{-1}) as a function of the daily runoff (mm day^{-1}), with points labelled by catchment and coloured based on their catchment average suspended sediment yield (Supplementary Table 1). Eight catchments have available daily runoff measurements, all shown here (Al = Alsea, Ca = Capesterre, Ch = Choshui, Ee = Eel, Er = Erlenbach, La = Langyang, Li = Liwu, Um = Umpqua). **B)** Rock-derived POC concentration, [POC_{petro}] (mg L^{-1}) versus daily runoff (mm day^{-1}), labelled the same as part **A**. Note, the Capesterre catchment has volcanic bedrock bearing no POC_{petro} and so does not appear on this plot, as do a number of points from the Umpqua River were POC_{petro} inputs were negligible. Grey filled symbols are catchments with no yield information. Uncertainties are derived from the mixing model outputs (Supplementary Table 4) and shown as grey whiskers if larger than the point size.

Figure 5: Daily runoff versus $POC_{biosphere}$ in forested mountain rivers. Concentration of POC eroded from the terrestrial biosphere, [$POC_{biosphere}$] (mg L^{-1}), as a function of daily runoff, R (mm day^{-1}), with points labelled by catchment (as per Fig. 4) and coloured based on their median slope angle. The variables are significantly correlated ($r = 0.53$, $P < 0.0001$, $n = 107$). Solid black line shows power law best fit to the data ([$POC_{biosphere}$] $= \alpha \cdot R^{\gamma}$, where $\alpha = 0.052 \pm 0.046$, $\gamma = 1.37 \pm 0.17$, $r^2 = 0.40$) with grey lines indicating the 95% confidence intervals. Solid lines show power law fits with modified α values, where red line has α x 3.4, and the orange line has α x 0.07, following the

discussion in the main text (Section 4.1.1). Uncertainties are derived from the mixing model outputs and shown as grey whiskers if larger than the point size.

Figure 6: Controls on annual $POC_{biosphere}$ yields. A) $POC_{biosphere}$ yield (tC km^{-2} yr^{-1}) as a function of suspended sediment yield (t km^{-2} yr^{-1}), with points labelled by catchment (as per previous figures, with additional data from He = Heping, Hu = Hualien, Cy = Chenyoulan, Hs = Hsiukuluan, Wu = Wulu, Ln = Laonung, Y = Yenping, Pn = Peinan, Lp = Linpien, Q = Quebrada, Ho = Hokitika, Ha = Haast, Wg = Wanganui, Po = Poerua, Wt = Waitangitaona, Wh = Whataroa, Wo = Waiho, F = Fox) and coloured based on annual runoff (grey when not available). Solid black line and grey lines show a power law fit to the data and 95% confidence interval. Dashed black line shows the global relationship following Galy et al., (2015). **B)** $POC_{biosphere}$ yield (tC km^{-2} yr^{-1}) as a function of mean annual runoff (m yr^{-1}), labelled by catchment and coloured by suspended sediment yield where available (grey where not). Power law fit to the data and 95% confidence bands are shown ($POC_{biosphere}$ yield = 7.6±3.0 x (Annual Runoff)$^{0.8\pm0.2}$, $r^2 = 0.31$, $n = 37$).

Figure 7: Shear-stress $POC_{biosphere}$ erosion model outputs. A) Mean annual $POC_{biosphere}$ yield (tC km^{-2} yr^{-1}) as a function of mean annual runoff (m yr^{-1}) with the catchment data shown as grey circles (from Fig. 6b). Model (Eq. 8) outputs for each year of historical data from the Liwu River (diamonds) and Eel River (squares) are shown. **B)** As part **A)**, but with the annual runoff variability (as relative standard deviation) for each year of the historical dataset used with the model outputs. **C)** The normalised distribution of daily runoff values in the historical datasets.

Figure 8: Modelled climate regulation of $POC_{biosphere}$ discharge. Outputs of shear-stress erosion model (Eq. 8) parameterised by the global dataset (Fig. 4). $POC_{biosphere}$ yield (tC km^{-2} yr^{-1}) is quantified as a function of annual runoff (mm yr^{-1}), keeping the variability of daily runoff values constant as defined by the Liwu River (Fig. 7c), while changing α (Eq. 10), $\Delta\alpha$, relative change from the value $\alpha = 0.052$ ($\Delta\alpha = 1$) defined by the global dataset (Fig. 5). α is a non-linear function of catchment-average slope (Eqs. 9 and 10).

Supplementary Table 1: Suspended sediment samples from global forested mountain rivers, with geochemical measurements of organic carbon concentration ([OC_{total}]), stable carbon isotope composition ($\delta^{13}C$), organic carbon to nitrogen ratio (C/N), fraction modern from radiocarbon (F_{mod}), daily runoff at the time of sample collection, suspended sediment concentration (SSC) and total POC concentration ([POC]). The biospheric POC concentration ([$POC_{biosphere}$]) and petrogenic POC concentration ([POC_{petro}]) and associated uncertainties are the result of mixing analyses described in the main text (and reported in Supplementary Table 4).

River	Lat.	Long.	Area km^2	[OC_{total}] %	$\delta^{13}C$ permil	C/N %/%	F_{mod}	Daily Runoff mm day^{-1}	SSC mg L^{-1}	[POC] mg L^{-1}	[$POC_{biosphere}$] mg L^{-1}	Error [$POC_{biosphere}$] mg L^{-1}	[POC_{petro}] mg L^{-1}	Error [POC_{petro}] mg L^{-1}	Reference
Peel	67.331	-134.866	70600	2.00	-26.8		0.38		250	5.0	3.5	0.7	1.54	0.74	Hilton et al., 2015
Peel	67.331	-134.866	70600	2.24	-26.8		0.28		101	2.3	1.6	0.3	0.62	0.30	Hilton et al., 2015
Peel	67.331	-134.866	70600	2.27	-26.8		0.48		325	7.4	5.4	1.0	2.01	0.97	Hilton et al., 2015
Peel	67.331	-134.866	70600	1.85	-26.6		0.31		146	2.7	1.8	0.4	0.90	0.43	Hilton et al., 2015
Arctic Red	67.439	-133.753	18600	2.17	-26.8		0.30		123	2.7	1.9	0.4	0.76	0.37	Hilton et al., 2015
Arctic Red	67.439	-133.753	18600	1.95	-26.8		0.29		123	2.4	1.6	0.4	0.76	0.37	Hilton et al., 2015
Erlenbach	47.045	8.709	0.74	2.04	-27.5	11.1	0.68	9.0	508	10.4	7.9	1.0	2.48	0.09	Smith et al., 2013
Erlenbach	47.045	8.709	0.74	1.14	-26.5	8.5	0.67	46.0	4128	47.2	35.4	4.3	11.81	0.09	Smith et al., 2013
Erlenbach	47.045	8.709	0.74	1.19	-26.2	8.7	0.47	60.3	1570	18.7	9.8	1.2	8.86	0.06	Smith et al., 2013
Erlenbach	47.045	8.709	0.74	2.08	-26.7	13.3	0.74	136.3	10344	214.8	177.9	21.8	36.97	0.10	Smith et al., 2013
Erlenbach	47.045	8.709	0.74	1.71	-26.7	12.0	0.69	240.8	8499	145.2	112.1	13.7	33.12	0.09	Smith et al., 2013
Erlenbach	47.045	8.709	0.74	1.62	-26.3	10.9	0.67	267.4	14063	228.5	171.3	21.0	57.22	0.09	Smith et al., 2013
Alsea	44.386	-123.831	1220	9.20	-25.1	9.3	1.01	4.5	4	0.4	0.4	0.0	0.01	0.01	Hatten et al., 2012
Alsea	44.386	-123.831	1220	2.60	-25.6	11.8	0.97	16.0	51	1.3	1.3	0.0	0.08	0.01	Hatten et al., 2012
Alsea	44.386	-123.831	1220	2.60	-25.3	13.0	1.00	29.7	71	1.8	1.8	0.0	0.06	0.01	Hatten et al., 2012
Alsea	44.386	-123.831	1220	5.20	-25.9	13.7	1.04	38.2	247	12.8	12.8	0.1	0.00	0.01	Hatten et al., 2012
Alsea	44.386	-123.831	1220	15.60	-26.5	16.1	1.03	4.5	1	0.2	0.2	0.0	0.00	0.01	Hatten et al., 2012
Alsea	44.386	-123.831	1220	3.80	-26.6	19.0	1.03	16.0	30	1.1	1.1	0.0	0.00	0.01	Hatten et al., 2012
Alsea	44.386	-123.831	1220	6.20	-26.5	19.4	1.03	29.7	156	9.7	9.6	0.1	0.03	0.01	Hatten et al., 2012
Alsea	44.386	-123.831	1220	7.60	-26.9	20.0	1.04	38.2	150	11.4	11.5	0.1	0.00	0.01	Hatten et al., 2012
Siuslaw	44.004	-124.006		6.74	-27.1	21.1	1.01								Leithold et al., 2006
Siuslaw	44.004	-124.006		4.86	-26.8	19.9	1.03								Leithold et al., 2006
Siuslaw	44.004	-124.006		5.43	-26.8	17.8	1.05								Leithold et al., 2006
Siuslaw	44.004	-124.006		7.11	-27.0	19.4	1.03								Leithold et al., 2006
Umpqua	43.586	-123.554	13000	8.11	-23.1	8.6	0.97	0.8	7	0.6	0.6	0.0	0.00	0.01	Goñi et al., 2013
Umpqua	43.586	-123.554	13000	4.76	-26.3	11.7	0.95	2.7	15	0.7	0.7	0.0	0.01	0.01	Goñi et al., 2013
Umpqua	43.586	-123.554	13000	3.34	-25.3	11.4	0.96	5.3	75	2.5	2.5	0.0	0.03	0.01	Goñi et al., 2013
Umpqua	43.586	-123.554	13000	2.62	-26.4	16.0	0.98	12.2	245	6.4	6.4	0.1	0.00	0.01	Goñi et al., 2013
Umpqua	43.586	-123.554	13000	2.63	-26.4	14.0	0.96	21.6	385	10.1	10.0	0.1	0.05	0.01	Goñi et al., 2013
Ishikari	43.219	141.660	14330	1.81	-30.6		0.64		369	6.7	4.3	0.3	2.40	0.04	Alam et al., 2007
Ishikari	43.219	141.660	14330	2.23	-26.4		0.83		88	2.0	1.6	0.0	0.32	0.02	Alam et al., 2007
Ishikari	43.219	141.660	14330	5.41	-27.8		0.90		6	0.3	0.3	0.0	0.03	0.03	Alam et al., 2007
Ishikari	43.219	141.660	14330	3.81	-28.5		0.84		11	0.4	0.3	0.0	0.07	0.03	Alam et al., 2007
Ishikari	43.219	141.660	14330	3.02	-25.9		0.83		22	0.7	0.6	0.0	0.11	0.03	Alam et al., 2007
Ishikari	43.219	141.660	14330	2.51	-30.6		0.78		22	0.6	0.4	0.0	0.12	0.03	Alam et al., 2007
Eel	40.492	-124.099	9537	0.90	-25.0	13.3	0.37								Leithold et al., 2006
Eel	40.492	-124.099	9537	1.00	-25.1	13.3	0.45								Leithold et al., 2006
Eel	40.492	-124.099	9537	1.09	-25.6	14.2	0.53								Leithold et al., 2006

Eel	40.492	-124.099	9537	0.76	-25.5	16.0	0.60								Leithold et al., 2006
Eel	40.492	-124.099	9537	1.06	-25.0	11.5	0.47								Leithold et al., 2006
Eel	40.492	-124.099	9537		-25.0		0.47								Leithold et al., 2006
Eel	40.492	-124.099	9537	0.99	-25.1	10.0	0.49	2.2	81	0.8	0.4	0.1	0.37	0.09	Goñi et al., 2013
Eel	40.492	-124.099	9537	0.83	-26.0	13.3	0.39	12.9	1072	8.9	3.8	0.7	5.13	0.07	Goñi et al., 2013
Eel	40.492	-124.099	9537	1.09	-26.4	12.2	0.56	19.6	3253	35.3	21.3	3.7	13.95	0.11	Goñi et al., 2013
Eel	40.492	-124.099	9537	0.81	-25.7	12.6	0.46	21.8	1909	15.4	7.7	1.3	7.72	0.09	Goñi et al., 2013
Noyo	39.426	-123.801		2.14	-26.2	21.9	0.78								Leithold et al., 2006
Noyo	39.426	-123.801		2.61	-26.1	15.3	1.00								Leithold et al., 2006
Noyo	39.426	-123.801		2.53	-26.4	16.2	0.98								Leithold et al., 2006
Noyo	39.426	-123.801		2.68	-26.5	20.0	0.98								Leithold et al., 2006
Noyo	39.426	-123.801		1.97	-26.2	19.9	0.95								Leithold et al., 2006
Navarro	39.197	-123.747		1.01	-25.5	15.4	0.74								Leithold et al., 2006
Navarro	39.197	-123.747		1.28	-25.5	10.8	0.72								Leithold et al., 2006
Navarro	39.197	-123.747		1.48	-25.8	14.3	0.83								Leithold et al., 2006
Navarro	39.197	-123.747		1.54	-26.2	14.0	0.84								Leithold et al., 2006
Navarro	39.197	-123.747		1.44	-26.0	14.9	0.88								Leithold et al., 2006
Navarro	39.197	-123.747		1.28	-25.9	16.4	0.81								Leithold et al., 2006
Navarro	39.197	-123.747		0.99	-25.8	15.1	0.76								Leithold et al., 2006
Santa Clara	34.235	-119.216	4210	0.94	-25.1		0.73								Komada et al., 2004
Santa Clara	34.235	-119.216	4210	1.11	-24.2		0.57								Komada et al., 2004
Santa Clara	34.235	-119.216	4210	3.44	-25.2		0.77								Komada et al., 2004
Santa Clara	34.235	-119.216	4210	1.76	-25.2		0.73								Komada et al., 2004
Santa Clara	34.235	-119.216	4210	1.01	-24.4		0.46								Komada et al., 2004
Santa Clara	34.235	-119.216	4210	1.37	-24.8		0.67								Komada et al., 2004
Santa Clara	34.235	-119.216	4210		-33.3		1.02								Masiello et al., 2001
Santa Clara	34.235	-119.216	4210	3.56	-25.3		0.87								Masiello et al., 2001
Santa Clara	34.235	-119.216	4210	1.60	-24.0		0.74								Masiello et al., 2001
Santa Clara	34.235	-119.216	4210	0.74	-19.7		0.35								Masiello et al., 2001
Santa Clara	34.235	-119.216	4210	1.15	-22.3		0.59								Masiello et al., 2001
Santa Clara	34.235	-119.216	4210	1.22	-20.6		0.47								Masiello et al., 2001
Karnali	28.642	81.283	57600	0.41	-25.6		0.83		1300	5.4	4.5	0.4	0.90	0.07	Galy and Eglinton, 2011
Karnali	28.642	81.283	57600	0.38	-25.4		0.78								Galy and Eglinton, 2011
Karnali	28.642	81.283	57600	0.33	-25.8		0.73								Galy and Eglinton, 2011
Karnali	28.642	81.283	57600	0.27	-25.9		0.70								Galy and Eglinton, 2011
Karnali	28.642	81.283	57600	0.28	-26.5		0.76								Galy and Eglinton, 2011
Narayani	27.703	84.427	31800	0.34	-24.5		0.39								Galy and Eglinton, 2011
Narayani	27.703	84.427	31800	0.33	-24.7		0.39		2900	9.5	9.2	1.8	0.38	0.19	Galy and Eglinton, 2011
Narayani	27.703	84.427	31800	0.21	-24.3		0.37		5600	12.0	11.0	2.1	1.02	0.18	Galy and Eglinton, 2011
Narayani	27.703	84.427	31800	0.18	-24.2		0.33		10200	18.4	15.0	2.9	3.46	0.16	Galy and Eglinton, 2011
Nayayani	27.703	84.427	31800	0.39	-23.9		0.31								Galy and Eglinton, 2011
Nayayani	27.703	84.427	31800	0.28	-24.4		0.49								Galy and Eglinton, 2011
Nayayani	27.703	84.427	31800	0.21	-24.0		0.45								Galy and Eglinton, 2011
Nayayani	27.703	84.427	31800	0.22	-23.9		0.43								Galy and Eglinton, 2011
Nayayani	27.703	84.427	31800	0.30	-24.0		0.48								Galy and Eglinton, 2011
Nayayani	27.703	84.427	31800	0.10	-23.7		0.15								Galy and Eglinton, 2011
Narayani	27.690	84.395	31800	0.22	-24.4		0.49								Galy and Eglinton, 2011
Kosi	26.847	87.152	51400	0.35	-25.1		0.84								Galy and Eglinton, 2011
Kosi	26.847	87.152	51400	0.32	-25.2		0.77		5700	18.2	16.5	1.0	1.72	0.05	Galy and Eglinton, 2011
Kosi	26.847	87.152	51400	0.42	-25.5		0.81		2600	10.8	10.4	0.6	0.42	0.06	Galy and Eglinton, 2011
Kosi	26.847	87.152	51400	0.05	-21.4		0.39								Galy and Eglinton, 2011
Kosi	26.847	87.152	51400	0.34	-26.0		0.81								Galy and Eglinton, 2011
Kosi	26.847	87.152	51400	0.42	-25.5		0.71								Galy and Eglinton, 2011

Kosi	26.847	87.152	51400	0.05	-23.7		0.25								Galy and Eglinton, 2011
Fonshan	24.851	121.015		0.67	-25.3		0.60		500	3.4	2.0	0.2	1.35	0.06	Kao et al., 2014
Langyang	24.715	121.772	820	0.68	-25.1		0.20	125.9	7700	52.4	10.4	1.1	41.93	0.02	Kao et al., 2014
Langyang	24.715	121.772	820	0.71	-25.4		0.29	268.7	24500	174.0	50.1	5.0	123.90	0.03	Kao et al., 2014
Langyang	24.715	121.772	820	0.58	-25.0		0.57	47.7	11400	66.1	37.7	3.8	28.47	0.06	Kao et al., 2014
Langyang	24.715	121.772	820	0.62	-25.3		0.71	164.4	6700	41.5	29.4	2.9	12.16	0.07	Kao et al., 2014
Langyang	24.715	121.772	820	0.58	-25.6		0.76	46.8	9800	56.8	43.4	4.3	13.44	0.08	Kao et al., 2014
Langyang	24.715	121.772	820	0.58	-25.7		0.78	67.6	5300	30.7	23.9	2.4	6.83	0.08	Kao et al., 2014
Langyang	24.715	121.772	820	1.03	-26.1		1.06	6.2	400	4.1	4.1	0.4	0.00	0.10	Kao et al., 2014
Liwu	24.179	121.492	435	0.41	-23.0		0.41	7.3	2500	10.3	4.2	0.4	6.08	0.04	Hilton et al., 2008a
Liwu	24.179	121.492	435	0.27	-21.8		0.10	25.0	13100	35.4	3.6	0.4	31.73	0.01	Hilton et al., 2008a
Liwu	24.179	121.492	435	0.38	-23.2		0.43	80.0	64200	244.0	104.4	10.5	139.55	0.04	Hilton et al., 2008a
Liwu	24.179	121.492	435	0.34	-23.7		0.08	38.7	24400	83.0	6.9	0.7	76.07	0.01	Hilton et al., 2008a
Liwu	24.179	121.492	435	0.39	-24.1		0.07	34.4	17600	68.6	5.1	0.5	63.56	0.01	Hilton et al., 2008a
Liwu	24.179	121.492	435	0.42	-24.4		0.05	8.7	7700	32.3	1.7	0.2	30.66	0.01	Hilton et al., 2008a
Liwu	24.179	121.492	435	0.37	-24.3		0.04	7.0	5800	21.5	0.9	0.1	20.52	0.01	Hilton et al., 2008a
Liwu	24.179	121.492	435	0.16	-22.5		0.17	17.3	30600	49.0	8.5	0.9	40.44	0.02	Hilton et al., 2008a
Liwu	24.179	121.492	435	0.28	-23.2		0.13	14.3	17700	49.6	6.3	0.7	43.22	0.01	Hilton et al., 2008a
Liwu	24.156	121.622	435	0.17	-24.1		0.40		59500	101.2	40.4	4.0	60.80	0.04	Kao et al., 2014
Liwu	24.156	121.622	435	0.12			0.30						0.00	0.03	Kao et al., 2014
Liwu	24.156	121.622	435	0.19	-23.8		0.36		83600	158.8	57.0	5.7	101.87	0.04	Kao et al., 2014
Liwu	24.156	121.622	435	0.15	-24.0		0.26		65100	97.7	25.0	2.5	72.66	0.03	Kao et al., 2014
Liwu	24.156	121.622	435	0.13	-24.0		0.30		43600	56.7	17.2	1.7	39.44	0.03	Kao et al., 2014
Liwu	24.156	121.622	435	0.20	-23.5		0.27		53000	106.0	28.9	2.9	77.06	0.03	Kao et al., 2014
Liwu	24.156	121.622	435	0.20	-23.9		0.11		34300	68.6	7.7	0.8	60.86	0.01	Kao et al., 2014
Liwu	24.156	121.622	435	0.30	-24.7		0.14		39600	118.8	16.6	1.7	102.16	0.01	Kao et al., 2014
Liwu	24.156	121.622	435	0.30	-24.7		0.09		30300	90.9	7.9	0.8	83.02	0.01	Kao et al., 2014
Wu	24.154	120.522		0.68	-24.7		0.56		3900	26.5	14.9	1.5	11.61	0.06	Kao et al., 2014
Choshui	23.810	120.469	2906	0.66	-24.5		0.24		6500	42.9	10.4	1.0	32.55	0.02	Kao et al., 2014
Choshui	23.785	120.636	2906	0.23	-26.6		0.19	95.1	199000	457.7	88.5	9.0	369.19	0.02	Kao et al., 2014
Choshui	23.785	120.636	2906	0.25	-25.4		0.33	74.9	87900	219.8	72.2	7.2	147.60	0.03	Kao et al., 2014
Choshui	23.785	120.636	2906	0.45	-25.6		0.52	190.0	11600	52.2	27.0	2.7	25.23	0.05	Kao et al., 2014
Choshui	23.784	120.885		0.63	-26.2		0.15		62800	395.6	60.2	6.1	335.47	0.02	Kao et al., 2014
Choshui	23.784	120.885		0.37	-26.0		0.13		41400	153.2	20.2	2.1	132.97	0.01	Kao et al., 2014
Choshui	23.784	120.885		0.32	-25.6		0.25		36600	117.1	28.8	2.9	88.34	0.02	Kao et al., 2014
Choshui	23.772	120.652		0.30	-26.2		0.31		133900	401.7	122.6	12.3	279.11	0.03	Kao et al., 2014
Choshui	23.772	120.652		0.25	-26.7		0.13		134200	335.5	43.3	4.4	292.25	0.01	Kao et al., 2014
Choshui	23.772	120.652		0.20	-26.4		0.12		132300	264.6	32.2	3.3	232.35	0.01	Kao et al., 2014
Choshui	23.695	120.852		0.32	-24.3		0.25		800	2.6	0.7	0.1	1.91	0.03	Kao et al., 2014
Choshui	23.695	120.852		0.29	-24.4		0.24		67500	195.8	47.5	4.8	148.24	0.02	Kao et al., 2014
Choshui	23.695	120.852		0.35	-25.1		0.67		83600	292.6	195.1	19.5	97.51	0.07	Kao et al., 2014
Tsengwen	23.108	120.205		0.49	-24.9		0.38		12900	63.2	24.0	2.4	39.19	0.04	Kao et al., 2014
Gaoping	22.770	120.454		0.58	-25.4		1.00		3600	20.9	20.8	2.1	0.07	0.10	Kao et al., 2014
Capesterre	16.072	-61.609	16.6	3.55		22.7		5.6	11	0.4	0.4				Lloret et al., 2013
Capesterre	16.072	-61.609	16.6	11.60		15.0		50.3	12	1.3	1.3				Lloret et al., 2013
Capesterre	16.072	-61.609	16.6	13.04		17.5		38.9	10	1.3	1.3				Lloret et al., 2013
Capesterre	16.072	-61.609	16.6	10.68		17.0		10.4	10	1.1	1.1				Lloret et al., 2013
Capesterre	16.072	-61.609	16.6	10.32		14.5		66.5	64	6.6	6.6				Lloret et al., 2013
Capesterre	16.072	-61.609	16.6	11.38		15.1		51.2	36	4.0	4.0				Lloret et al., 2013
Capesterre	16.072	-61.609	16.6	17.18		11.3		46.8	19	3.3	3.3				Lloret et al., 2013
Capesterre	16.072	-61.609	16.6	15.54		18.7		52.3	18	2.8	2.8				Lloret et al., 2013
Capesterre	16.072	-61.609	16.6	9.60		12.7		34.5	81	7.7	7.7				Lloret et al., 2013
Capesterre	16.072	-61.609	16.6	8.29		12.6		23.9	74	6.1	6.1				Lloret et al., 2013

Capesterre	16.072	-61.609	16.6	12.34	16.3	19.1	55	6.8	6.8	Lloret et al., 2013
Capesterre	16.072	-61.609	16.6	10.57	14.8	15.8	36	3.8	3.8	Lloret et al., 2013
Capesterre	16.072	-61.609	16.6	12.12	16.9	11.6	25	3.1	3.1	Lloret et al., 2013
Capesterre	16.072	-61.609	16.6	12.96	16.4	10.8	21	2.7	2.7	Lloret et al., 2013
Capesterre	16.072	-61.609	16.6	18.01	26.7	17.4	10	1.8	1.8	Lloret et al., 2013
Capesterre	16.072	-61.609	16.6	14.15	16.1	31.5	25	3.5	3.5	Lloret et al., 2013
Capesterre	16.072	-61.609	16.6	22.92	31.2	19.1	6	1.3	1.3	Lloret et al., 2013
Capesterre	16.072	-61.609	16.6	10.65	16.4	103.4	63	6.7	6.7	Lloret et al., 2013
Capesterre	16.072	-61.609	16.6	15.17	22.9	38.1	14	2.1	2.1	Lloret et al., 2013
Capesterre	16.072	-61.609	16.6	11.39	16.0	109.8	105	11.9	11.9	Lloret et al., 2013
Capesterre	16.072	-61.609	16.6	12.79	14.3	90.1	154	19.7	19.7	Lloret et al., 2013
Capesterre	16.072	-61.609	16.6	12.82	14.0	73.8	87	11.2	11.2	Lloret et al., 2013
Capesterre	16.072	-61.609	16.6	13.37	13.1	54.8	56	7.4	7.4	Lloret et al., 2013
Capesterre	16.072	-61.609	16.6	15.79	12.6	46.6	34	5.4	5.4	Lloret et al., 2013
Capesterre	16.072	-61.609	16.6	13.26	13.3	41.1	28	3.8	3.8	Lloret et al., 2013
Capesterre	16.072	-61.609	16.6	23.51	9.0	19.4	7	1.5	1.5	Lloret et al., 2013
Capesterre	16.072	-61.609	16.6	8.72	19.8	49.4	44	3.8	3.8	Lloret et al., 2013
Capesterre	16.072	-61.609	16.6	12.36	14.5	45.3	50	6.2	6.2	Lloret et al., 2013
Capesterre	16.072	-61.609	16.6	11.20	16.1	39.9	54	6.0	6.0	Lloret et al., 2013
Capesterre	16.072	-61.609	16.6	11.17	16.8	32.7	41	4.6	4.6	Lloret et al., 2013
Capesterre	16.072	-61.609	16.6	10.48	13.1	29.4	34	3.6	3.6	Lloret et al., 2013
Capesterre	16.072	-61.609	16.6	11.12	15.3	27.6	25	2.8	2.8	Lloret et al., 2013
Capesterre	16.072	-61.609	16.6	9.82	17.0	63.2	42	4.2	4.2	Lloret et al., 2013
Capesterre	16.072	-61.609	16.6	11.47	15.4	32.2	21	2.4	2.4	Lloret et al., 2013
Capesterre	16.072	-61.609	16.6	7.62	18.5	98.6	36	2.7	2.7	Lloret et al., 2013
Capesterre	16.072	-61.609	16.6	7.43	15.9	101.1	52	3.9	3.9	Lloret et al., 2013
Capesterre	16.072	-61.609	16.6	6.36	12.5	104.6	46	2.9	2.9	Lloret et al., 2013
Capesterre	16.072	-61.609	16.6	5.94	12.8	107.6	49	2.9	2.9	Lloret et al., 2013
Capesterre	16.072	-61.609	16.6	9.99	18.4	110.7	55	5.5	5.5	Lloret et al., 2013
Capesterre	16.072	-61.609	16.6	7.35	27.2	77.4	45	3.3	3.3	Lloret et al., 2013
Capesterre	16.072	-61.609	16.6	8.53	17.7	325.6			0.0	Lloret et al., 2013
Capesterre	16.072	-61.609	16.6	10.83	24.0	104.3	61	6.6	6.6	Lloret et al., 2013
Capesterre	16.072	-61.609	16.6	3.81	43.0	51.1	31	1.2	1.2	Lloret et al., 2013
Capesterre	16.072	-61.609	16.6	12.75	14.1	57.7	38	4.9	4.9	Lloret et al., 2013
Capesterre	16.072	-61.609	16.6	12.11	13.7	54.6	43	5.2	5.2	Lloret et al., 2013
Capesterre	16.072	-61.609	16.6	11.08	12.6	51.5	41	4.6	4.6	Lloret et al., 2013
Capesterre	16.072	-61.609	16.6	11.45	13.6	48.4	43	4.9	4.9	Lloret et al., 2013
Capesterre	16.072	-61.609	16.6	10.76	15.0	45.3	38	4.0	4.0	Lloret et al., 2013
Capesterre	16.072	-61.609	16.6	9.96	14.3	42.2	23	2.3	2.3	Lloret et al., 2013
Capesterre	16.072	-61.609	16.6	10.99	13.3	128.0	94	10.4	10.4	Lloret et al., 2013
Capesterre	16.072	-61.609	16.6	13.41	13.4	77.0	81	10.9	10.9	Lloret et al., 2013
Capesterre	16.072	-61.609	16.6	13.35	14.1	63.4	67	8.9	8.9	Lloret et al., 2013
Capesterre	16.072	-61.609	16.6	10.57	13.4	47.9	54	5.7	5.7	Lloret et al., 2013
Capesterre	16.072	-61.609	16.6	9.97	13.2	41.9	47	4.7	4.7	Lloret et al., 2013
Capesterre	16.072	-61.609	16.6	9.26	14.1	36.7	34	3.1	3.1	Lloret et al., 2013
Capesterre	16.072	-61.609	16.6	8.58	14.7	30.2	30	2.6	2.6	Lloret et al., 2013
Capesterre	16.072	-61.609	16.6	7.35	12.6	28.0	34	2.5	2.5	Lloret et al., 2013
Capesterre	16.072	-61.609	16.6	7.34	12.6	33.2	22	1.6	1.6	Lloret et al., 2013
Capesterre	16.072	-61.609	16.6	15.71	15.2	103.9	476	74.8	74.8	Lloret et al., 2013
Capesterre	16.072	-61.609	16.6	10.17	13.6	85.7	248	25.2	25.2	Lloret et al., 2013
Capesterre	16.072	-61.609	16.6	13.19	13.4	70.8	161	21.2	21.2	Lloret et al., 2013
Capesterre	16.072	-61.609	16.6	12.53	13.4	59.7	132	16.5	16.5	Lloret et al., 2013
Capesterre	16.072	-61.609	16.6	14.94	13.8	50.8	61	9.1	9.1	Lloret et al., 2013

Capesterre	16.072	-61.609	16.6	12.84		12.8		44.6	70	9.0	9.0				Lloret et al., 2013
Capesterre	16.072	-61.609	16.6	13.23		13.7		37.1	191	26.0	26.0				Lloret et al., 2013
Ucayali	-8.783	-74.553	205520	1.24	-28.1		0.93		289	3.6	3.3	0.3	0.27	0.09	Mayorga et al., 2005
Ucayali	-8.783	-74.553	205520		-28.6		1.04			0.7	0.7	0.1	0.00	0.10	Mayorga et al., 2005
Urubamba	-10.757	-73.712	61070	1.67	-27.1		0.70		269	4.5	3.2	0.3	1.34	0.07	Mayorga et al., 2005
Urubamba	-10.757	-73.712	61070		-28.5		1.08			1.0	1.0	0.1	0.00	0.10	Mayorga et al., 2005
Tambo	-10.787	-73.773	121290	1.47	-27.6		0.93		251	3.7	3.4	0.3	0.25	0.09	Mayorga et al., 2005
Tambo	-10.787	-73.773	121290		-28.3		1.09			0.1	0.1	0.0	0.00	0.10	Mayorga et al., 2005
Urubamba	-12.867	-72.682	12640	2.73	-24.3		0.92		55	1.5	1.4	0.1	0.13	0.09	Mayorga et al., 2005
Urubamba	-12.867	-72.682	12640		-26.2		1.02			0.0	0.0	0.0	0.00	0.10	Mayorga et al., 2005
Kosnipata (San Pedro)	-13.058	-71.544	161	0.86	-26.3	6.1	0.51		299	2.6	1.3	0.1	1.28	0.06	Clark et al., 2013
Kosnipata (San Pedro)	-13.058	-71.544	161	0.64	-24.6	4.6	0.38		371	2.4	0.9	0.1	1.48	0.04	Clark et al., 2013
Kosnipata (San Pedro)	-13.058	-71.544	161	0.80	-25.9	5.7	0.41		340	2.7	1.1	0.1	1.62	0.05	Clark et al., 2013
Kosnipata (San Pedro)	-13.058	-71.544	161	0.86	-25.6	5.7	0.59		7594	65.3	37.6	4.2	27.70	0.06	Clark et al., 2013
Kosnipata (San Pedro)	-13.058	-71.544	161	0.81	-25.5	5.1	0.50		1531	12.4	6.1	0.7	6.34	0.05	Clark et al., 2013
Kosnipata (San Pedro)	-13.058	-71.544	161	0.80	-25.2	5.0	0.53		1212	9.7	5.0	0.6	4.67	0.06	Clark et al., 2013
Kosnipata (San Pedro)	-13.058	-71.544	161	0.57	-24.5	4.1	0.29		938	5.3	1.5	0.2	3.82	0.03	Clark et al., 2013
Kosnipata (San Pedro)	-13.058	-71.544	161	0.59	-24.6	4.2	0.30		636	3.8	1.1	0.1	2.65	0.03	Clark et al., 2013
Kosnipata (San Pedro)	-13.058	-71.544	161	0.67	-25.1	5.2	0.58		226	1.5	0.9	0.1	0.65	0.06	Clark et al., 2013
Kosnipata (San Pedro)	-13.058	-71.544	161	6.83	-30.3	34.2	0.99		105	7.2	7.0	0.8	0.17	0.11	Clark et al., 2013
Kosnipata (San Pedro)	-13.058	-71.544	161	1.09	-26.3	6.8	0.88		180	2.0	1.7	0.2	0.26	0.10	Clark et al., 2013
Kosnipata (San Pedro)	-13.058	-71.544	161	0.52	-24.9	4.3	0.31		889	4.6	1.4	0.2	3.22	0.03	Clark et al., 2013
Kosnipata (Wayqecha)	-13.163	-71.589	50	0.74	-25.9	5.7	0.55		137	1.0	0.6	0.1	0.43	0.07	Clark et al., 2013
Kosnipata (Wayqecha)	-13.163	-71.589	50	1.18	-27.0	7.9	0.67		113	1.3	0.9	0.1	0.40	0.08	Clark et al., 2013
Kosnipata (Wayqecha)	-13.163	-71.589	50	1.03	-26.2	5.4	0.79		1891	19.5	16.2	1.9	3.26	0.10	Clark et al., 2013
Kosnipata (Wayqecha)	-13.163	-71.589	50	1.30	-26.1	6.5	0.81		1696	22.0	18.8	2.2	3.22	0.10	Clark et al., 2013
Kosnipata (Wayqecha)	-13.163	-71.589	50	0.76	-26.1	5.4	0.71		2869	21.8	16.4	1.9	5.40	0.09	Clark et al., 2013
Kosnipata (Wayqecha)	-13.163	-71.589	50	0.62	-25.6	4.8	0.60		737	4.6	2.9	0.3	1.68	0.07	Clark et al., 2013
Kosnipata (Wayqecha)	-13.163	-71.589	50	0.85	-26.7	5.7	0.65		136	1.2	0.8	0.1	0.36	0.08	Clark et al., 2013
Kosnipata (Wayqecha)	-13.163	-71.589	50	0.94	-26.2	6.7	0.67		78	0.7	0.5	0.1	0.21	0.08	Clark et al., 2013
Apurimac	-13.567	-72.589	22760	8.84	-23.7		1.03		7	0.6	0.6	0.1	0.00	0.10	Mayorga et al., 2005
Apurimac	-13.567	-72.589	22760		-23.8		0.99			0.0	0.0	0.0		0.10	Mayorga et al., 2005
Salcca	-14.102	-71.422	3190	1.15	-24.6		0.39		290	3.3	1.3	0.1	2.03	0.04	Mayorga et al., 2005
Salcca	-14.102	-71.422	3190		-25.9		0.80			6.6	5.3	0.5	1.35	0.08	Mayorga et al., 2005
Vilcanota	-14.166	-71.402	1610	16.16	-24.6		0.75		5	0.7	0.5	0.1	0.18	0.07	Mayorga et al., 2005
Vilcanota	-14.166	-71.402	1610		-26.4		0.65			0.0	0.0	0.0		0.07	Mayorga et al., 2005
Zongo	-16.253	-68.118	260	0.73	-25.6		0.78		95	0.7	0.5	0.1	0.15	0.08	Mayorga et al., 2005
Zongo	-16.253	-68.118	260		-27.6		1.06								Mayorga et al., 2005
Waiapu	-37.894	178.295	1378	0.71	-25.3	11.8	0.18								Leithold et al., 2006
Waiapu	-37.894	178.295	1378	0.54	-25.4	13.1	0.26								Leithold et al., 2006
Waiapu	-37.894	178.295	1378	0.50	-25.2	12.7	0.30								Leithold et al., 2006
Waiapu	-37.894	178.295	1378	0.72	-25.2	12.0	0.19								Leithold et al., 2006
Waiapu	-37.894	178.295	1378	0.55	-25.4	11.6	0.24								Leithold et al., 2006
Waiapu	-37.894	178.295	1378	0.59	-25.6	12.0	0.28								Leithold et al., 2006
Waiapu	-37.894	178.295	1378	0.60	-25.4	12.4	0.28								Leithold et al., 2006
Waipaoa	-38.462	177.876	1580	0.44	-26.4	12.7	0.40								Leithold et al., 2006
Waipaoa	-38.462	177.876	1580	0.64	-26.1	12.3	0.48								Leithold et al., 2006
Waipaoa	-38.462	177.876	1580	0.72	-26.3	11.8	0.51								Leithold et al., 2006
Waipaoa	-38.462	177.876	1580	0.82	-26.7	11.8	0.74								Leithold et al., 2006

Supplementary Table 2: Global forested mountain river catchments with estimates of suspended sediment and $POC_{biosphere}$, and POC_{petro} yields, and annual runoff.

River Catchment	Label	Lat.	Long.	Area km^2	Yield method	POC method[a]	Years	Annual Runoff m yr^{-1}	Suspended sediment yield t km^{-2} yr^{-1}	$POC_{biosphere}$ yield tC km^{-2} yr^{-1}	POC_{petro} yield tC km^{-2} yr^{-1}	Reference
Arctic Red	AR	67.439	-133.753	18600	Spot samples	1	N/A	0.3	392	5.7	2.4	Hilton et al., 2015
Peel	Pe	67.331	-134.866	70600	Spot samples	1	N/A	0.3	295	4.3	1.8	Hilton et al., 2015
Erlenbach	Er	47.045	8.709	0.74	Frequent sampling	2	1983-2011	2.2	1648	14.0	10.1	Smith et al., 2013
Alsea	Al	44.386	-123.831	1220	Frequent sampling	1	2008	1.5	53	3.8	0.0	Hatten et al. 2012
Siuslaw	Si	44.004	-124.006	1523	Spot samples	1	N/A	1.4	128	7.7	0.0	Leithold et al. 2006
Umpqua	Um	43.586	-123.554	13000	Frequent sampling	1	2008-2009	0.7	31	1.0	0.0	Goñi et al., 2013
Eel	Ee	40.492	-124.099	9537	Frequent sampling	1	2008-2009	0.8	224	1.0	1.0	Goñi et al., 2013
Eel	Ee	40.492	-124.099	8063	Spot samples	1	N/A	1.5	1720	8.6	7.9	Leithold et al. 2006
Noyo	No	39.426	-123.801	293	Spot samples	1	N/A	1.6	234	5.3	0.2	Leithold et al. 2006
Navarro	Na	39.197	-123.747	816	Spot samples	1	N/A	1.1	683	6.7	2.1	Leithold et al. 2006
Santa Clara	SC	34.235	-119.216	4210	Spot samples	1	1998	0.4	1621	14.9	6.1	Hatten et al. 2012
Karnali	Ka	28.642	81.283	57600	Spot samples	1	2002-2011		2257	5.9	1.2	Galy et al., 2015
Narayani	Ny	27.703	84.427	31800	Spot samples	1	2002-2011	1.6	3459	5.5	2.5	Galy et al., 2015
Kosi	Ko	26.847	87.152	51400	Spot samples	1	2002-2011		2529	5.1	0.8	Galy et al., 2015
Langyang	La	24.715	121.772	820	Frequent sampling	2	1993-1994	2.2	7800	4.9	18.1	Kao and Liu, 2000
Heping	He	24.326	121.735	553	Frequent sampling	3	2005-2006	2.9	18704	9.3	79.6	Hilton et al. 2011a
LiWu	Li	24.179	121.492	435	Frequent sampling	3	2004	2.2	18571	6.8	47.6	Hilton et al. 2011a
Hualien	Hu	23.924	121.591	1506	Frequent sampling	3	2005-2006	3.8	25292	13.8	69.5	Hilton et al. 2011a
Choshui	Ch	23.789	120.628	2906	Frequent sampling	3	2005-2006	2.3	22798	20.8	101.3	Hilton et al. 2011a
Chenyoulan	Cy	23.715	120.838	367	Frequent sampling	3	2005-2006	2.7	21064	19.6	58.3	Hilton et al. 2011a
Hsiukuluan	Hs	23.487	121.397	1539	Frequent sampling	3	2005-2006	2.2	4061	1.2	19.2	Hilton et al. 2011a
Wulu	Wu	23.124	121.157	639	Frequent sampling	3	2005-2006	2.5	10344	13.8	22.9	Hilton et al. 2011a
Laonung	Ln	23.050	120.661	812	Frequent sampling	3	2005-2006	4.1	4399	4.3	11.6	Hilton et al. 2011a
Yenping	Y	22.900	121.077	476	Frequent sampling	3	2005-2006	4.6	58897	23.4	245.6	Hilton et al. 2011a
Peinan	Pn	22.793	121.134	1584	Frequent sampling	3	2005-2006	2.5	72993	74.4	227.9	Hilton et al. 2011a
Linpien	Lp	22.464	120.542	310	Frequent sampling	3	2005-2006	3.1	2909	2.8	13.4	Hilton et al. 2011a
Capesterre	Ca	16.072	-61.609	16.6	Frequent sampling	4	2007-2010	4.0	153	18.3	0.0	Lloret et al., 2013
Quebrada Mariposa	Q	8.717	-83.617	0.094	Frequent sampling	4	2009	1.1	151	17.8	0.0	Taylor et al., 2015
Waiapu	Wa	-37.894	178.295	1734	Spot samples	1	N/A	2.3	20000	29.7	90.6	Leithold et al. 2006
Waipaoa	Wp	-38.462	177.876	2205	Spot samples	1	N/A	2.0	6800	23.7	20.8	Leithold et al. 2006
Hokitika	Ho	-42.746	170.999	352	Spot samples	2	N/A	8.9	6313	38.0	9.0	Hilton et al., 2008b
Haast	Ha	-42.855	169.054	1020	Spot samples	2	N/A	5.8	4500	9.0	6.0	Hilton et al., 2008b
Wanganui	Wg	-43.155	170.625	344	Spot samples	2	N/A		12500	37.0	19.0	Hilton et al., 2008b
Poerua	Po	-43.157	170.504	136	Spot samples	2	N/A		26200	52.0	39.0	Hilton et al., 2008b
Waitangitaona	Wt	-43.283	170.307	72	Spot samples	2	N/A	5.9	12500	64.0	19.0	Hilton et al., 2008b
Whataroa	Wh	-43.285	170.403	453	Spot samples	2	N/A	9.5	10325	87.0	15.0	Hilton et al., 2008b
Waiho	Wo	-43.393	170.181	164	Spot samples	2	N/A		10325	12.0	15.0	Hilton et al., 2008b
Fox	F	-43.478	170.008	92	Spot samples	2	N/A		12500	18.0	19.0	Hilton et al., 2008b

[a]Method used to quantify $POC_{biosphere}$ and POC_{petro} contributions: 1 = ^{14}C; 2 = $\delta^{13}C$; 3 = $\delta^{13}C$, N/C and ^{14}C; 4 = not applicable, volcanic bedrock

Supplementary Table 3: Geomorphic characteristics of mountain river catchments from 3 arc-second digital elevation model to quantify 16th, 50th and 84th percentiles of slope angle (θ, degrees) and elevation (Z, meters) in catchments where daily runoff measurements are available.

River Catchment	Label	Lat.	Long.	Area	θ_{16}	θ_{50}	θ_{84}	Z_{16}	Z_{50}	Z_{84}
				km^2	°	°	°	m	m	m
Alsea	Al	44.386	-123.831	1220	8	17	26	145	289	491
Umpqua	Um	43.586	-123.554	13000	7	16	26	292	675	1200
Eel	Ee	40.492	-124.099	9537	9	17	24	403	707	1201
Langyang	La	24.715	121.772	820	5	23	33	204	838	1664
LiWu	Li	24.179	121.492	435	20	30	39	1348	2042	2707
Choshui	Ch	23.789	120.628	2906	12	26	37	655	1542	2473
Chenyoulan	Cy	23.715	120.838	367	17	30	38	967	1634	2376
Capesterre	Ca	16.072	-61.609	16.6	9	18	31	450	770	1035

Supplementary Table 4: Outputs of binary mixing model (Eq. 1-4), with the fraction modern of the biosphere-derived POC ($F_{mod-bio}$) and petrogenic content ($[OC_{petro}]$) and associated propagated uncertainty. The r^2 describes the goodness of fit between the binary mixing model (Eq. 4) and the data, and the P value the significance of the fit.

River	Lat.	Long.	$F_{mod-bio}$	Error $F_{mod-bio}$	$[OC_{petro}]$ %	Error $[OC_{petro}]$ %	r^2	P
Erlenbach	47.045	8.709	0.89	0.11	0.42	0.21	0.93	0.0012
Alsea	44.386	-123.831	1.03	0.01	0.06	0.07	0.99	<0.0001
Siuslaw	44.004	-124.006	0.98	0.06	0.28	0.36	0.99	0.0034
Umpqua	43.586	-123.554	0.97	0.01	0.00	0.06	0.99	<0.0001
Ishikari	43.219	141.660	1.00	0.04	0.54	0.13	0.99	<0.0001
Eel	40.492	-124.099	0.93	0.16	0.44	0.18	0.91	0.0168
Noyo	39.426	-123.801	1.34	0.29	0.71	0.55	0.83	0.0194
Navarro	39.197	-123.747	1.04	0.11	0.30	0.14	0.94	0.0002
Santa Clara	34.235	-119.216	0.94	0.04	0.42	0.08	0.98	<0.0001
Karnali	28.642	81.283	0.99	0.09	0.08	0.03	0.97	0.0013
Narayani	27.703	84.427	0.40	0.08	0.00	0.05	0.72	0.0006
Kosi	26.847	87.152	0.85	0.05	0.03	0.02	0.98	<0.0001
Kosnipata (San Pedro)	-13.058	-71.544	1.02	0.11	0.41	0.10	0.92	0.0001
Kosnipata (Wayqecha)	-13.163	-71.589	0.95	0.11	0.25	0.11	0.92	0.0001

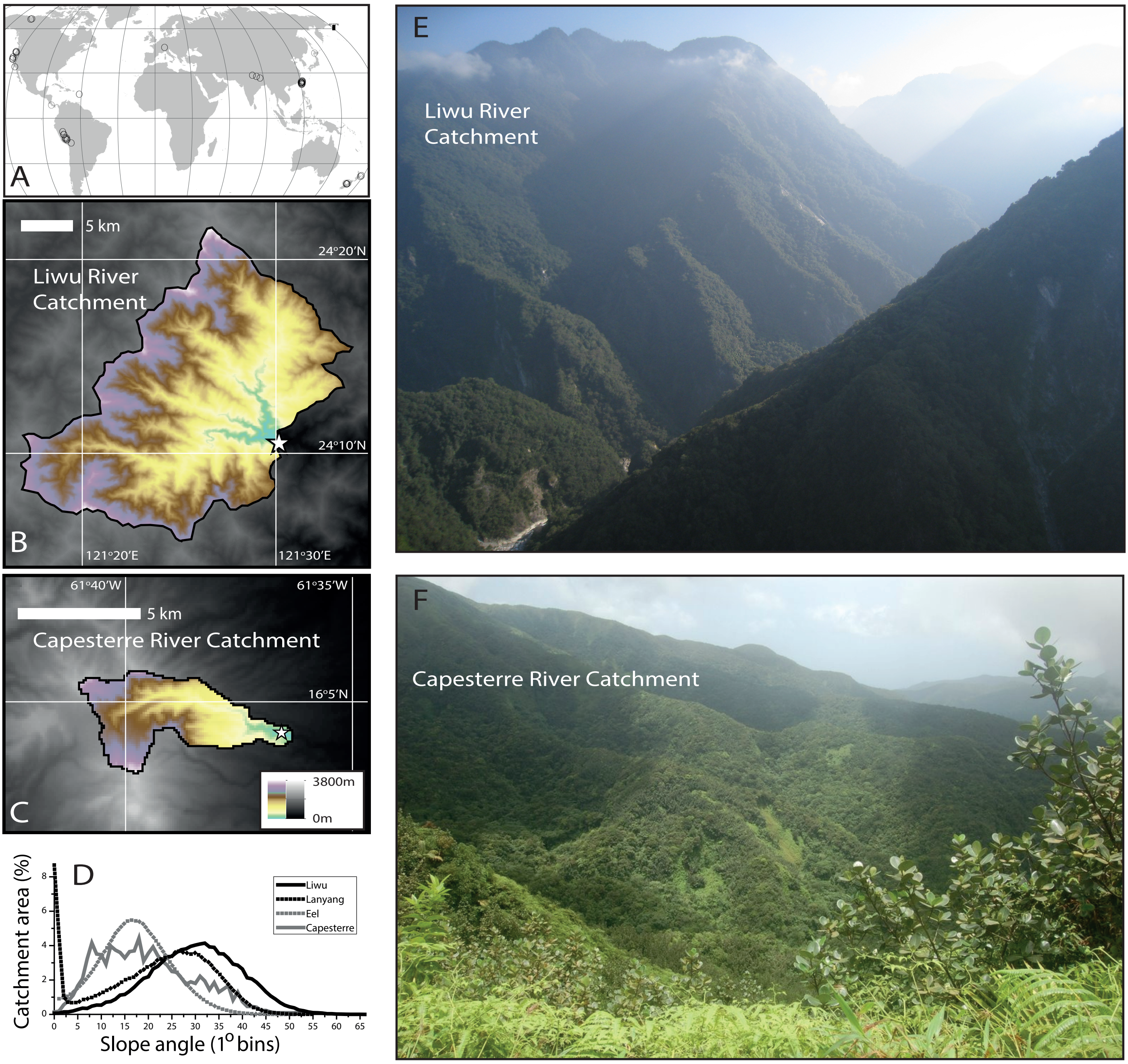
A
5 km
Liwu River
Catchment
24°20'N
24°10'N
B
121°20'E
121°30'E
61°40'W
61°35'W
5 km
Capesterre River Catchment
16°5'N
3800m
0m
C
D
Catchment area (%)
Slope angle (1° bins)
Liwu
Lanyang
Eel
Capesterre
E
Liwu River
Catchment
F
Capesterre River Catchment

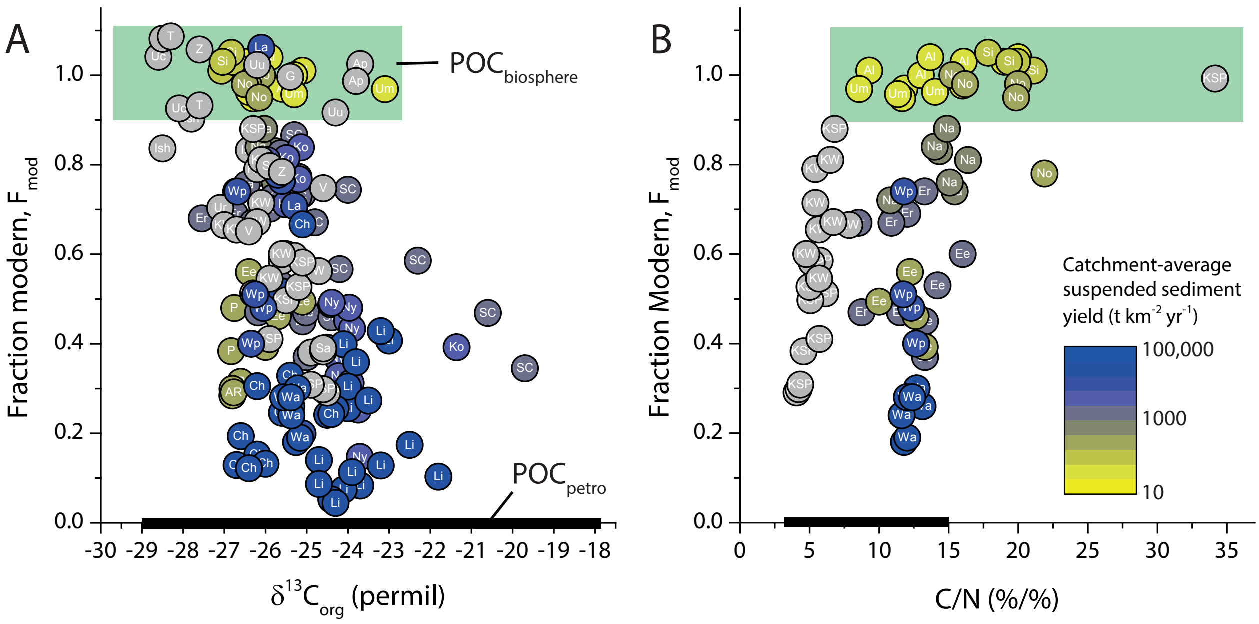
A
B
POC$_{biosphere}$
POC$_{petro}$
Fraction modern, F_{mod}
Fraction Modern, F_{mod}
$\delta^{13}C_{org}$ (permil)
C/N (%/%)
Catchment-average suspended sediment yield (t km^{-2} yr^{-1})
100,000
1000
10

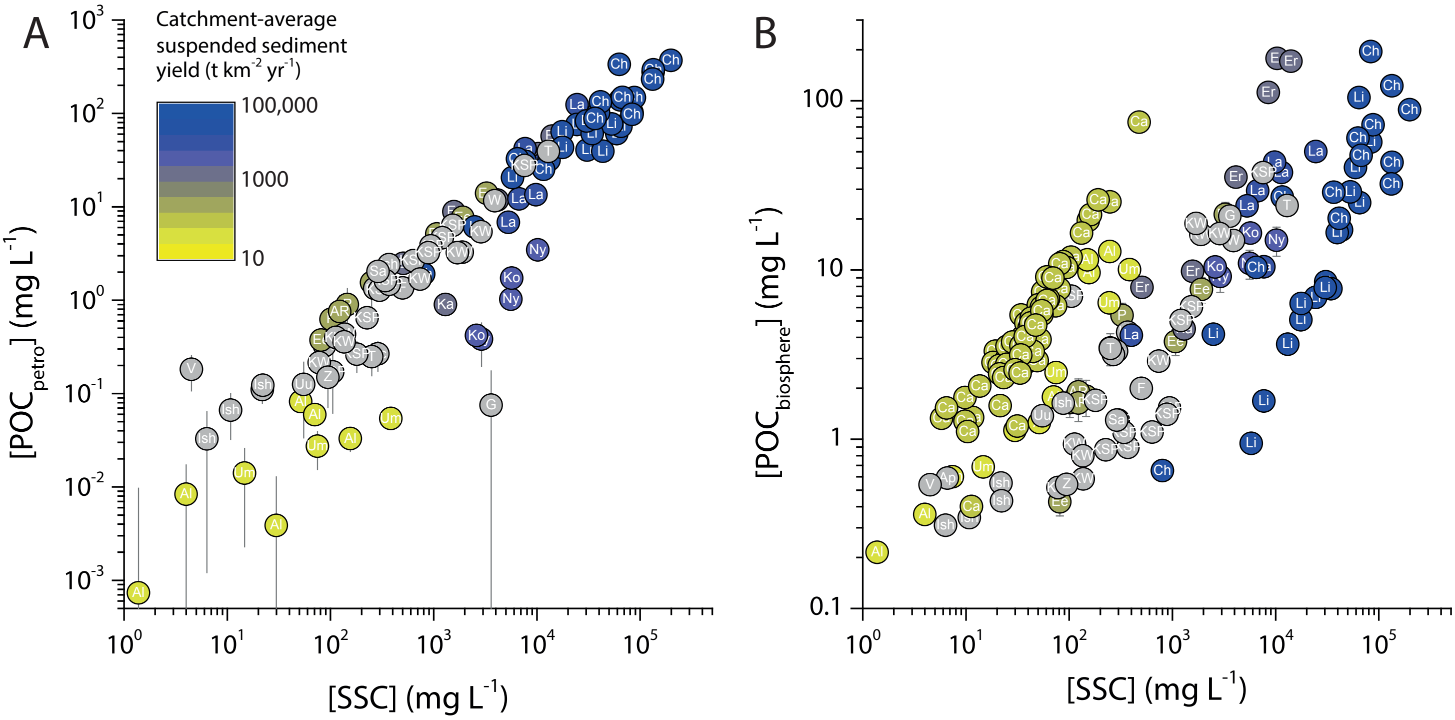
A
B
Catchment-average suspended sediment yield (t km^{-2} yr^{-1})
100,000
1000
10
[POC_{petro}] (mg L^{-1})
[$POC_{biosphere}$] (mg L^{-1})
[SSC] (mg L^{-1})
10^{-3}
10^{-2}
10^{-1}
10^{0}
10^{1}
10^{2}
10^{3}
10^{4}
10^{5}
0.1
1
10
100

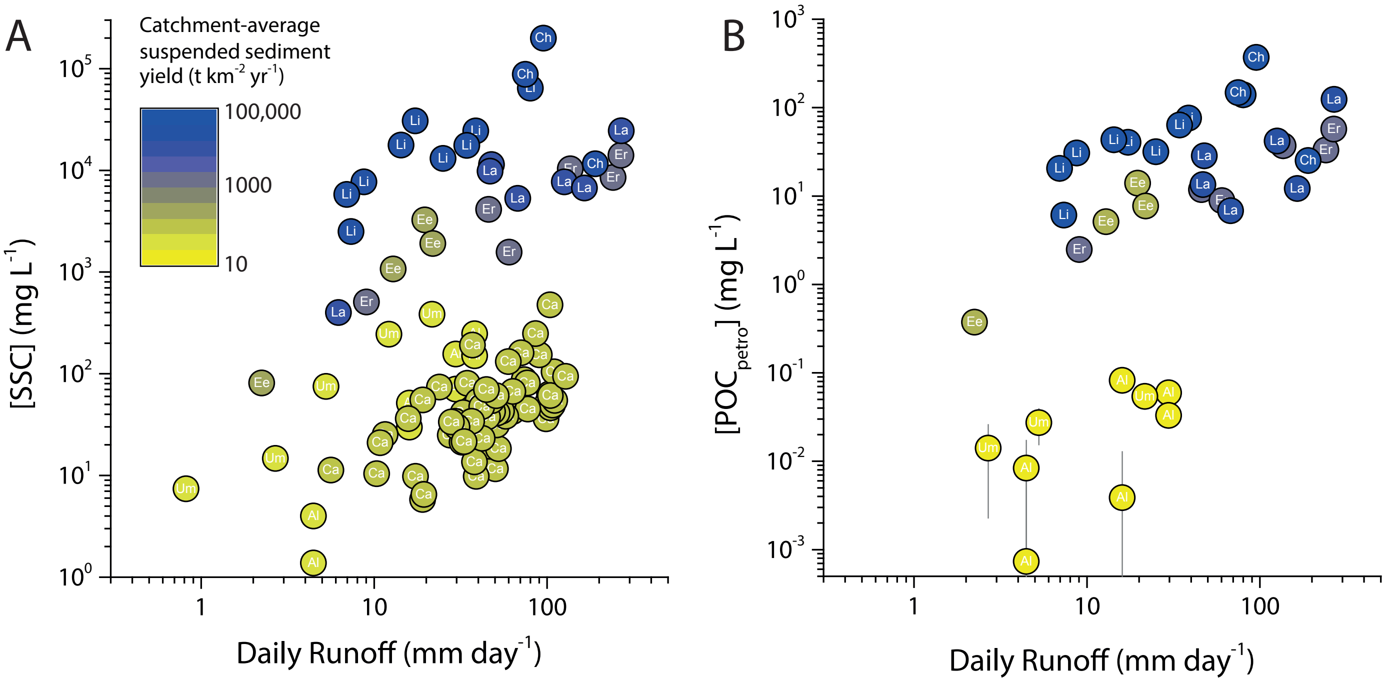
A
Catchment-average suspended sediment yield (t km-2 yr-1)
100,000
1000
10
[SSC] (mg L-1)
Daily Runoff (mm day-1)
B
[POCpetro] (mg L-1)
Daily Runoff (mm day-1)

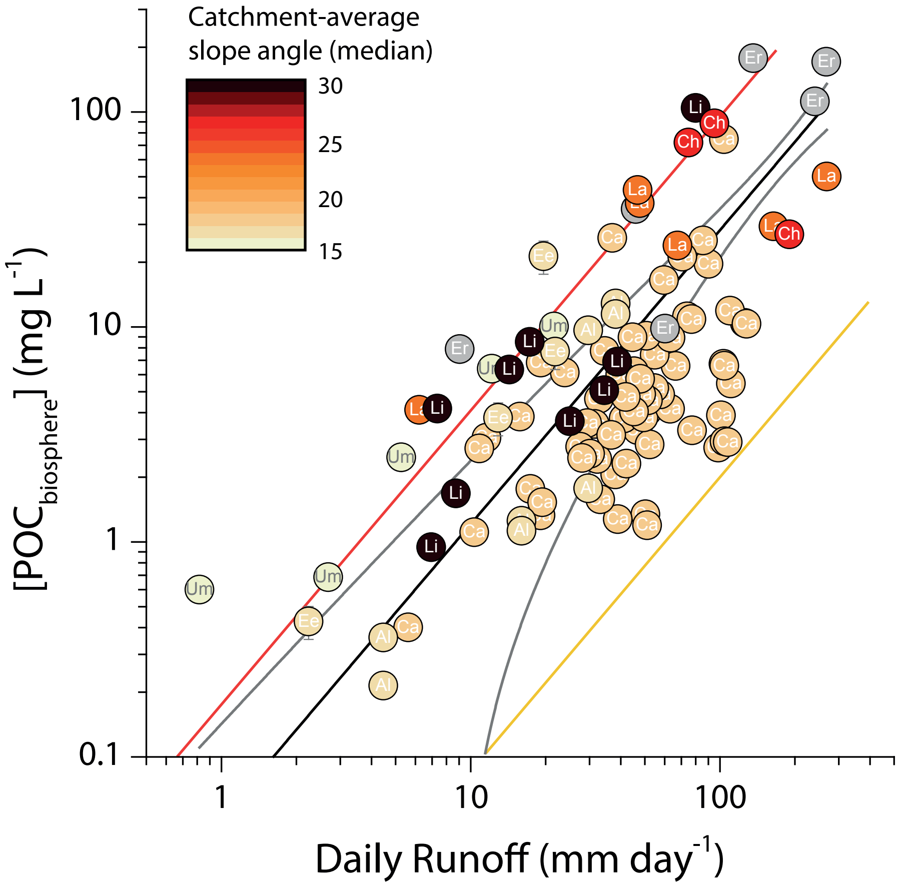

Catchment-average
slope angle (median)
30
25
20
15
100
10
1
0.1
[POC$_{biosphere}$] (mg L^{-1})
1
10
100
Daily Runoff (mm day^{-1})

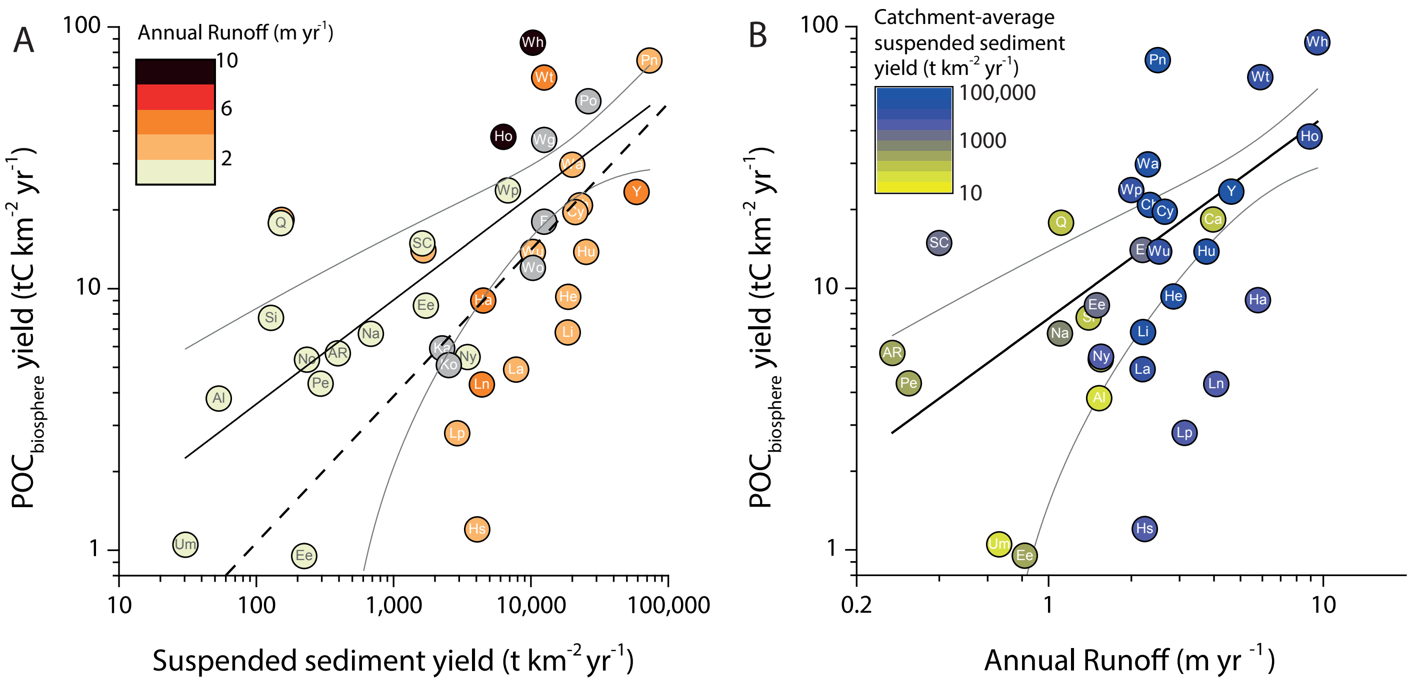
A
B
Annual Runoff (m yr-1)
10
6
2
Catchment-average suspended sediment yield (t km-2 yr-1)
100,000
1000
10
POCbiosphere yield (tC km-2 yr-1)
Suspended sediment yield (t km-2 yr-1)
Annual Runoff (m yr-1)
100
10
1
10
100
1,000
10,000
100,000
0.2
1
10

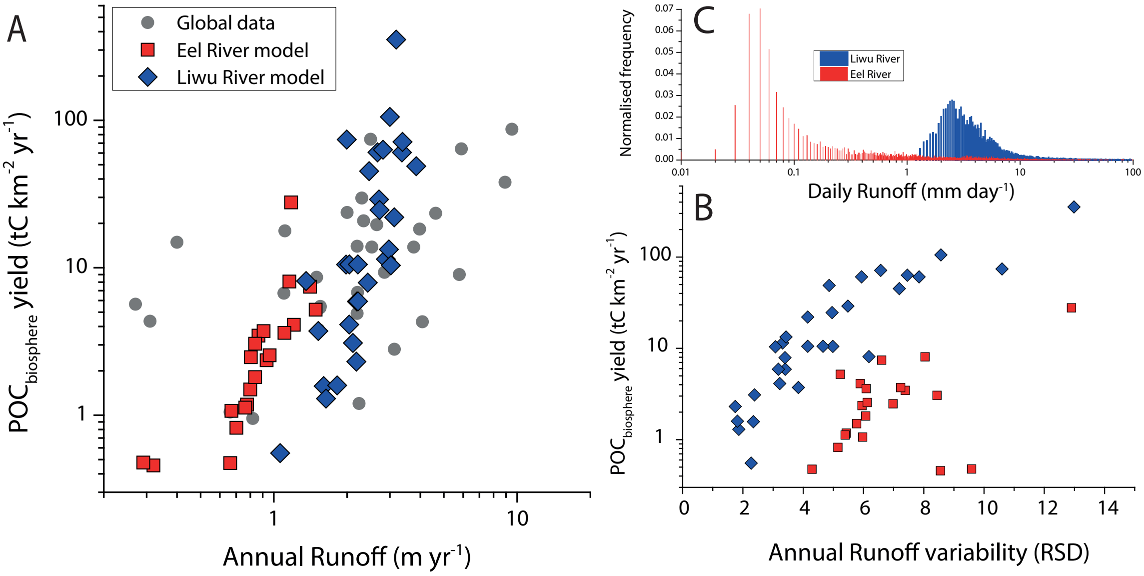

A
Global data
Eel River model
Liwu River model
POC$_{biosphere}$ yield (tC km^{-2} yr^{-1})
Annual Runoff (m yr^{-1})
C
Normalised frequency
Liwu River
Eel River
Daily Runoff (mm day^{-1})
B
POC$_{biosphere}$ yield (tC km^{-2} yr^{-1})
Annual Runoff variability (RSD)

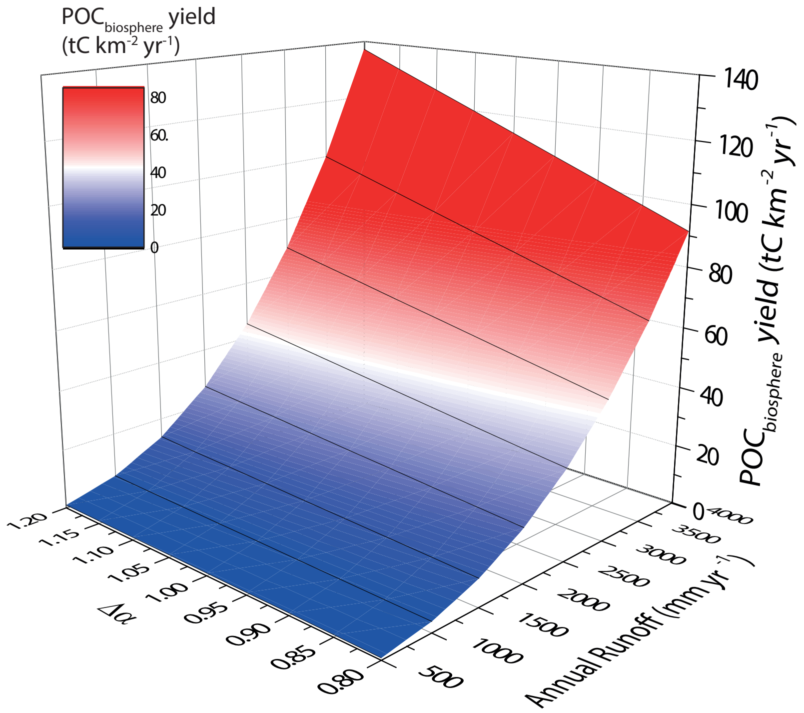

POC$_{biosphere}$ yield
(tC km^{-2} yr^{-1})
80
60.
40
20
0
140
120
100
80
60
40
20
0
POC$_{biosphere}$ yield (tC km^{-2} yr^{-1})
1.20
1.15
1.10
1.05
1.00
0.95
0.90
0.85
0.80
Δα
4000
3500
3000
2500
2000
1500
1000
500
Annual Runoff (mm yr^{-1})